

Certifiably Optimal Estimation and Calibration in Robotics via Trace-Constrained Semi-Definite Programming

Liangting Wu and Roberto Tron

Abstract—Many nonconvex problems in robotics can be relaxed into convex formulations via Semi-Definite Programming (SDP) that can be solved to global optimality. The practical quality of these solutions, however, critically depends on rounding them to rank-1 matrices, a condition that can be challenging to achieve. In this work, we focus on trace-constrained SDPs (TCSDPs), where the decision variables are Positive Semi-Definite (PSD) matrices with fixed trace values. We show that the latter can be used to design a gradient-based refinement procedure that projects relaxed SDP solutions toward rank-1, low-cost candidates. We also provide fixed-trace SDP relaxations for common robotic quantities such as rotations, translations, and a modular virtual robot abstraction that simplifies modeling across different problem settings. We demonstrate that our trace-constrained SDP framework can be applied to many robotics tasks, and we showcase its effectiveness through simulations in Perspective-n-Point (PnP) estimation, hand-eye calibration, and dual-robot system calibration.

I. Introduction

SDP relaxation. Many problems in robotics can be encoded as a Polynomial Optimization Problem (POP), where the objective function and constraints are polynomials of the variables. It is well known that such problems are generally non-convex and can be hard to solve optimally. A common approach is via Semi-Definite Relaxations (SDRs), where a relaxed convex problem is solved. This is typically done by constructing a lifted vector \mathbf{x} using the variables and a moment matrix $\mathbf{M} = \mathbf{x}\mathbf{x}^\top$ such that the objective function and constraints in the POP are linear functions of \mathbf{M} . SDRs have been popular because:

- (i) Relaxations are convex, and can generally be solved with many off-the-shelf solvers.
- (ii) The Lagrangian dual of the SDP can provide a certificate of global optimality [25], [26].

Tightness of SDR. In general, a solution \mathbf{x} to the original POP can be only extracted when $\mathbf{M} = \mathbf{x}\mathbf{x}^\top$, i.e., when $\text{rank}(\mathbf{M}) = 1$ [10]; however, this condition is typically dropped in the SDR to make the relaxation convex. There exist special cases, such as when the number of constraints is less than 2, for which solutions to the SDR are also rank-1 [2], [17], [18]; in this case the SDR is said to be tight. Many works investigate techniques for making SDR tight by adding redundant constraints to the relaxed SDP [4], [25]; these constraints

The authors are with the Department of Mechanical Engineering, Boston University, 110 Cummington Mall, MA 02215, United States tomwu@bu.edu, tron@bu.edu. The authors gratefully acknowledge the support by NSF award FRR-2212051.

are redundant in the original POP, but enforce internal structures on the moment matrix that are lost during the relaxation. Lassere's hierarchy [9] provides a way to systematically make a POP SDR tight with a finite (but possibly quite large) number of additional variables and constraints [16]. In [4], the redundant constraints are found automatically by computing the nullspace of a data matrix obtained from using feasible samples.

Scalability. In practice, SDP solvers do not scale favorably with the size of the moment matrix \mathbf{M} . It is therefore important to use sparsity to reduce the size of the problem when many of the entries in \mathbf{M} do not appear in the original POP [20], [21].

Trace-constrained SDP. There exists some work exploring the role of constant-trace constraints [8], [27] for tightness and for obtaining rank-1 solutions. With constant trace, the SDP with rank-1 constraint can be cast as an eigenvalue optimization problem, enabling the use of gradients of eigenvalues to project solutions onto the rank-1 set. In [14], it is shown that any POP with a ball constraint can be relaxed to an SDP with a constant trace constraint.

The present paper generalizes and provides a more systematic approach to our previous work on Trace-Constrained SDP relaxations for problems in Inverse Kinematics [22], [23], and Visual Inverse Kinematics [24]. In particular, we extend the framework to estimation and calibration problems that were not considered in those works. We additionally provide a larger library of relaxations for common quantities in robotics, in some instances (e.g., distance-and-direction constraints), using smaller SDP embedding. Compared to previous work on TCSDP (e.g., [13], [14]), we provide specific formulations tailored to robotics problems.

Paper contributions. Our key contributions include:

- We introduce constant-trace semidefinite variables for relaxations of rotation matrices $\text{SO}(3)$ and translations $\mathbb{R} \times \mathcal{S}^2$, which are tightened using structural constraints in addition to the trace constraint, and show that the original manifold variables can be exactly recovered when these constant-trace variables are rank-1.
- We provide additional techniques based on ideas from Control Barrier Functions (CBF) to accelerate the solver of [23], which, unlike the original method, can recover solutions that are not only low-rank but also low-cost.
- We introduce the SP robot, a virtual kinematic

module that models diverse robotics problems, and show that solving its kinematics yields optimal solutions for PnP estimation, hand-eye calibration, and dual-robot calibration problems.

II. Preliminaries

A. Notation

Vectors and matrices are denoted by bold-face lowercase and uppercase letters. The reference frames are denoted by sans-serif letters. The operator $\text{tr}(\cdot)$ denotes the trace. A PSD matrix is denoted by $\succeq 0$. A list of notations is in Table I.

w	World reference frame
$b_1 \mathbf{R}_{b_2}$	Rotation matrix from reference frame b_2 to b_1
$b_1 \mathbf{t}_{b_2}$	Translation from reference frame b_2 to b_1
$b_1 \mathbf{T}_{b_2}$	Rigid transformation from reference frame b_2 to b_1
\mathbf{R}_{b_2}	Rotation from frame b_2 to the world frame
$\mathbf{R}^{(i)}$	The i -th column of the matrix \mathbf{R}
\mathbf{K}	Camera intrinsic matrix
$\mathbf{M}(a : b, c : d)$	Block in matrix \mathbf{M} for rows a to b and columns c to d
$\{\mathbf{v}_i\}_n$	A set of members consisting $\mathbf{v}_1, \dots, \mathbf{v}_n$
$\text{stack}(\{\mathbf{v}_i\}_n)$	The vertical concatenation of all the members within $\{\mathbf{v}_i\}_n$
$\text{vec}(\mathbf{M})$	Vectorization, $\text{stack}(\{\text{vec}(\mathbf{M}_i)\}_n)$ when $\mathbf{M} = \{\mathbf{M}_i\}_n$
$\lambda_1(\mathbf{M})$	Largest eigenvalue of \mathbf{M} ,
\mathbb{S}_+^d	$\sum_i^n \{\lambda_1(\mathbf{M}_i)\}_n$ when $\mathbf{M} = \{\mathbf{M}_i\}_n$
$\text{SO}(d)$	Space of $d \times d$ positive semi-definite matrices
\mathcal{S}^n	Special orthogonal group in dimension d
f^*	The n -sphere: $\mathcal{S} = \{\mathbf{x} \in \mathbb{R}^{n+1} \mid \ \mathbf{x}\ _2^2 = 1\}$
	An optimal cost of function f

TABLE I: Table of notations

B. SDP Relaxations

Define $\mathbf{Y} = \{\mathbf{Y}_i \mid \mathbf{Y}_i \in \mathbb{S}_+^{d_{y,i}}\}_{n_y}$ as a collection of matrices. Denote $N = \dim(\text{vec}(\mathbf{Y}))$. Given $\mathbf{Q} \succeq 0$, $\mathbf{c}, \mathbf{a}_j \in \mathbb{R}^N$, consider the following quadratic SDP:

Problem 1 (Trace-Constrained Relaxed SDP):

$$\min_{\mathbf{Y}=\{\mathbf{Y}_i\}_{n_y}} f(\mathbf{Y}) := \mathbf{y}^\top \mathbf{Q} \mathbf{y} + \mathbf{c}^\top \mathbf{y} \quad (1a)$$

$$\text{s.t. } \mathbf{a}_j^\top \mathbf{y} = b_j, \quad j = 1, \dots, n_e, \quad (1b)$$

$$\text{tr}(\mathbf{Y}_i) = \bar{\lambda}, \quad i \in \{1, \dots, n_y\}, \quad (1c)$$

$$\mathbf{Y}_i \in \mathbb{S}_+^{d_{y,i}}, \quad i \in \{1, \dots, n_y\}, \quad (1d)$$

where $\{d_{y,i}\}$, n_y , and n_e are the dimensions of the embedding, the number of variables, and the number of constraints. The matrix \mathbf{Y}_i is positive semi-definite with a constant trace $\bar{\lambda}$.

Unlike standard SDP formulations, the constant-trace constraint (1c) bounds the largest eigenvalue λ_1 of \mathbf{Y}_i , linking rank-1 conditions to maximizing λ_1 (see Section III-A).

We now convert Problem 1 into standard form. Define $\mathcal{A}(\mathbf{Y}) = \mathbf{b}$ as the linear operator of all linear (including the trace) constraints in Problem 1 and its adjoint $\mathcal{A}^* : \langle \mathcal{A}^*(\rho), \mathbf{Y} \rangle := \sum_{i=1}^n \langle (\mathcal{A}^*(\rho))_i, \mathbf{Y}_i \rangle$. Decompose $\mathbf{Q} = \mathbf{L}^\top \mathbf{L}$, define the expression $\mathbf{y} := \text{vec}(\mathbf{Y})$, and write the following standard form SDP equivalent to Problem 1.

Problem 2 (Primal, standard form SDP):

$$\min_{\{\mathbf{Y}_i \succeq 0\}, t} t + \mathbf{c}^\top \mathbf{y} \quad (2a)$$

$$\text{s.t. } \mathcal{A}(\mathbf{Y}) = \mathbf{b}, \quad \mathbf{Y}_i \succeq 0 \quad \forall i, \quad (2b)$$

$$\begin{bmatrix} t & (\mathbf{L}\mathbf{y})^\top \\ \mathbf{L}\mathbf{y} & \mathbf{I} \end{bmatrix} \succeq 0. \quad (2c)$$

The epigraph variable $t \in \mathbb{R}$ and (2c) imply $t \geq \mathbf{y}^\top \mathbf{Q} \mathbf{y}$. Define $\mathcal{V}^* : \langle \mathcal{V}^*(\mathbf{r}), \mathbf{Y} \rangle = \mathbf{r}^\top \text{vec}(\mathbf{Y})$. The dual problem of Problem 2 is

Problem 3 (Dual SDP):

$$\max_{\rho, \mathbf{S}=\{\mathbf{S}_i\}, \mathbf{Z}} d(\rho, \mathbf{Z}) := \rho^\top \mathbf{b} - \text{tr}(\mathbf{Z}) + 1 \quad (3a)$$

$$\text{s.t. } \mathbf{Z} = \begin{bmatrix} 1 & \mathbf{z}^\top \\ \mathbf{z} & \mathbf{Z}_{22} \end{bmatrix}, \quad (3b)$$

$$\mathcal{V}^*(\mathbf{c} - 2\mathbf{L}^\top \mathbf{z}) = \mathcal{A}^*(\rho) + \mathbf{S}, \quad (3c)$$

$$\mathbf{S}_i \succeq 0 \quad \forall i = 1, \dots, n_y, \quad (3d)$$

where $\rho \in \mathbb{R}^{n_e}$, \mathbf{Z}, \mathbf{S} are dual variables. See the Appendix for the derivation.

It is well known that $f^* \geq d^*$ holds and $f^* - d^*$ is called the duality gap. For a feasible solution $(\hat{\mathbf{Y}}, \hat{t})$, we can certify its optimality directly by the Karush–Kuhn–Tucker (KKT) conditions. In particular, if there exist dual variables $(\hat{\rho}, \{\hat{\mathbf{S}}_i\}, \hat{\mathbf{Z}})$ such that

$$\left\langle \hat{\mathbf{Z}}, \begin{bmatrix} \hat{t} & (\hat{\mathbf{L}}\hat{\mathbf{y}})^\top \\ \hat{\mathbf{L}}\hat{\mathbf{y}} & \mathbf{I} \end{bmatrix} \right\rangle = 0, \quad \left\langle \hat{\mathbf{S}}_i, \mathbf{Y}_i^* \right\rangle = 0, \quad \forall i = 1, \dots, n_y; \quad (4a)$$

$$\hat{\mathbf{S}}_i \succeq 0 \quad \forall i, \quad \hat{\mathbf{Z}} \succeq 0, \quad (4b)$$

where $\hat{\mathbf{y}} := \text{vec}(\hat{\mathbf{Y}})$, then strong duality holds and the primal and dual optimal values coincide. In this case, the duality gap is zero and $(\hat{\mathbf{Y}}, \hat{t})$ is a global optimal solution.

III. Rank and Cost Optimization of TCSDP

In this section, we present a rank minimization method to project relaxed SDP solutions onto rank-1 matrices, followed by a cost-reduction method for rank-1 solutions.

A. A gradient-based approach for rank minimization

This subsection discusses the rank minimization strategy from [22] that applies to any fixed-trace matrix.

For a PSD matrix $\mathbf{M} \in \mathbb{S}_+^d$ with fixed trace, $\text{rank}(\mathbf{M}) = 1$ if and only if

$$\mathbf{M} = \text{argmax}(\lambda_1(\mathbf{M})), \quad (5)$$

where $\lambda_1(\cdot)$ indicates the largest eigenvalue of its matrix argument. Intuitively, since the trace is also the sum of eigenvalues, the sum $\sum_{l=1}^d \lambda_l(\mathbf{M})$ is also fixed. This implies that when λ_1 is maximized, we have $\lambda_l(\mathbf{M}) = 0, \forall l = 2, \dots, d$, hence \mathbf{M} is rank-1; see [22] for a proof.

Using (5), we can project a matrix \mathbf{M} to the rank-1 set by increasing $\lambda_1(\mathbf{M})$. Fortunately, the function $\lambda_1(\mathbf{M})$ is differentiable on \mathbf{M} (so long as $\lambda_1(\mathbf{M})$ has multiplicity 1) and the gradient $\nabla \lambda_1(\mathbf{M})$ can be computed [12, Theorem 1]. This enables the projected gradient-descent approach of [22] which increases $\lambda_1(\mathbf{M})$ by solving the following SDP at every iteration:

Problem 4 (Rank Minimization Update):

$$\min_{\Delta \mathbf{Y}^k, c} f(\mathbf{Y}^{k-1} + \Delta \mathbf{Y}^k) + \gamma_c c \quad (6a)$$

$$\text{s.t. } \text{vec}(\Delta \mathbf{Y}^k)^\top \nabla \lambda_1(\mathbf{Y}^{k-1}) \geq (c-1)(\lambda_1(\mathbf{Y}^{k-1}) - \bar{\lambda}_s) \quad (6b)$$

$$c \in [0, 1] \quad (6c)$$

$$\mathbf{Y}_i^{k-1} + \Delta \mathbf{Y}_i^k \in \mathcal{Y}, \forall i = 1, \dots, n_y \quad (6d)$$

The scalar γ_c is a weight factor, and $\bar{\lambda}_s$ is the sum of the fixed trace value for all \mathbf{Y}_i . The constraint \mathcal{Y} is the feasible set (1b)-(1d). The solution to (6) computes an increment $\Delta \mathbf{Y}^k$ such that $\mathbf{Y}^k = \Delta \mathbf{Y}^k + \mathbf{Y}^{k-1}$. The constraints (6b) and (6c) imply that the concave function $\bar{\lambda}_s - \lambda_1(\mathbf{Y}^k)$ decreases at a geometric rate [23, Sec. VII.D]. Problem 4 tries to find the update that minimizes the cost subject to the constraints, but the latter take precedence; as a result, it might not converge to a constrained minimizer of f .

B. Low-rank channel

As shown in [23], [24], solving a sequence of Problem 4 often yields solutions satisfying $\bar{\lambda}_s - \sum_i^{n_y} \lambda_1(\mathbf{Y}_i) \approx 0$, i.e., approximately rank-1 under a given tolerance. However, such rank-1 solutions are not necessarily optimal. In practice, the cost $f(\mathbf{Y})$ typically increases during rank minimization (6), with the rate of increase influenced by the weight γ_c . Moreover, applying Problem 4 to reduce cost after reaching the rank-1 set leads to only minor improvements, since the updates effectively attempt linear movements along a curved boundary defined by (6b), without leaving the boundary itself.

To account for the above limitations, we provide a novel iterative approach to find a low-cost solution while maintaining the rank-1 property.

We note two observations. (i) It is well known that the optimal solution \mathbf{Y}^* is also rank-1. (ii) The rank-1 set is on the boundary of the feasible set (6d) (this is because the boundary of the PSD cone is the singular matrices).

Our strategy is to move \mathbf{Y} along the rank-1 set while minimizing the cost towards \mathbf{Y}^* by introducing a parameter γ in Problem 4.

Problem 5: (Low-rank channel update)

$$\min_{\Delta \mathbf{Y}^k, c} f(\mathbf{Y}^{k-1} + \Delta \mathbf{Y}^k) \quad (7a)$$

$$\text{s.t. } \text{vec}(\Delta \mathbf{Y}^k)^\top \nabla \lambda_1(\mathbf{Y}^{k-1}) \geq (c-1)(\lambda_1(\mathbf{Y}^{k-1}) - \gamma \bar{\lambda}_s) \quad (7b)$$

$$(6c) \text{ and } (6d) \quad (7c)$$

Problem 5 aims to find a solution such that the updated matrices are close to rank-1, summarized in the following proposition.

Proposition 1: Given $\gamma \in (0, 1)$ and a \mathbf{Y}^{k-1} that satisfies $\lambda_1(\mathbf{Y}^{k-1}) \geq \gamma \bar{\lambda}_s$, for an optimal solution $\Delta \mathbf{Y}^k$ of Problem 5, we have

$$\gamma \bar{\lambda}_s \leq \lambda_1(\mathbf{Y}^{k-1} + \Delta \mathbf{Y}^k) \leq \bar{\lambda}_s. \quad (8)$$

Proof: We start with the first inequality of (8).

Inspired by concepts in Control-Barrier-Function (CBF), we define

$$h(\mathbf{Y}) := \lambda_1(\mathbf{Y}) - \gamma \bar{\lambda}_s \quad (9)$$

For a sequence $\{\mathbf{Y}^k\}$ and $h(\mathbf{Y}^0) \geq 0$, we have $h(\mathbf{Y}^k) \geq 0, \forall k \in \mathbb{Z}^+$ if the following condition holds [1][Prop. 4].

$$\Delta h(\mathbf{Y}^k) + b h(\mathbf{Y}^{k-1}) \geq 0, \forall k \in \mathbb{Z}^+, b \in (0, 1]. \quad (10)$$

Substitute (9) into (10) for \mathbf{Y}^{k-1} and \mathbf{Y}^k to get

$$\lambda_1(\mathbf{Y}^k) - \lambda_1(\mathbf{Y}^{k-1}) + b(\lambda_1(\mathbf{Y}^{k-1}) - \gamma \bar{\lambda}_s) \geq 0 \quad (11)$$

Because $\lambda_1(\mathbf{Y})$ is a convex function, we have

$$\lambda_1(\mathbf{Y}^k) \geq \lambda_1(\mathbf{Y}^{k-1}) + \text{vec}(\Delta \mathbf{Y}^k)^\top \nabla \lambda_1(\mathbf{Y}^{k-1}) \quad (12)$$

Using (12), $\lambda_1(\mathbf{Y}^{k-1}) > 0$, $\lambda_1(\mathbf{Y}^k) > 0$, and $b h(\mathbf{Y}^{k-1}) \geq 0$, we have

$$\text{vec}(\Delta \mathbf{Y}^k)^\top \nabla \lambda_1(\mathbf{Y}^{k-1}) + b(\lambda_1(\mathbf{Y}^{k-1}) - \gamma \bar{\lambda}_s) \geq 0 \Rightarrow (11). \quad (13)$$

Replace b with $c \in [0, 1]$, the l.h.s. of (13) is exactly (7b). The implication holds when $c = 1$. Thus $h(\mathbf{Y}^k) \geq 0$ and the left inequality holds when (7b) and (7c) hold for \mathbf{Y}^{k-1} .

The second inequality of (8) is enforced by the constant-trace and the PSD constraints. ■

Proposition 1 establishes that the sum of the largest eigenvalues of the updated solution lies between the bounds in (7b) and (7c), thereby defining a low-rank channel of width determined by γ within which the solution can be steered toward lower cost.

Tolerance Scheduling. Iteratively solving Problem 5 improves the cost, but progress can be slow when the rank-minimized solution is far from low-cost; to address this, we propose replacing constraint (7b) with (14) to more efficiently reduce the cost of a rank-1 solution.

$$\text{vec}(\Delta \mathbf{Y}^k)^\top \nabla \lambda_1(\mathbf{Y}^{k-1}) \geq (c-1)(\lambda_1(\mathbf{Y}^{k-1}) - \bar{\lambda}_s) - \sigma^k. \quad (14)$$

For $\bar{\sigma} > 0$, we define a decreasing tolerance sequence σ^k for the rank reduction constraint (6b) that reaches $\bar{\sigma}$ in finite steps. Unlike Problem 5, which strictly bounds the rank, tolerance scheduling uses the soft constraint (14) to gradually reduce rank while allowing cost-reducing updates of larger magnitude. In practice, scheduling can be combined with the low-rank channel: first moving a rank-1 solution to a low-cost region, then fine-tuning with the channel. An example σ^k and simulations are presented in Section VII.

IV. Trace-Constrained SDP Relaxations

In this section, we show how fixed-trace PSD matrices can represent both rotation matrices and rigid translations.

A. Relaxation of $\text{SO}(3)$

We start with a brief review of a relaxation of $\text{SO}(3)$ originally introduced in [22].

Consider a problem with n_y rotation matrices as variables. For each rotation matrix $\mathbf{R}_i \in \text{SO}(3)$, we define a decision variable \mathbf{Y}_i .

Definition 1: A matrix \mathbf{Y}_i can be built from \mathbf{R}_i as

$$\mathbf{Y}_i = \begin{bmatrix} \mathbf{R}_i^{(1)} \\ \mathbf{R}_i^{(2)} \\ 1 \end{bmatrix} \begin{bmatrix} \mathbf{R}_i^{(1)} \\ \mathbf{R}_i^{(2)} \\ 1 \end{bmatrix}^\top \in \mathbb{R}^{7 \times 7}. \quad (15)$$

We define the constraint $\mathbf{Y}_i \in \mathcal{Y}$ as

$$\text{tr}(\mathbf{Y}_i(1:3, 1:3)) = \text{tr}(\mathbf{Y}_i(4:6, 4:6)) = 1 \quad (16a)$$

$$\text{tr}(\mathbf{Y}_i(1:3, 4:6)) = 0 \quad (16b)$$

$$\mathbf{Y}_i(7, 7) = 1 \quad (16c)$$

$$\mathbf{Y}_i \succeq 0 \quad (16d)$$

The matrix \mathbf{Y}_i contains all elements of $\mathbf{R}_i^{(1),(2)}$, $\mathbf{R}_i^{(1)}$. $\mathbf{R}_i^{(2)}$, which are used in (16a)-(16c) to enforce $\mathbf{R}_i^{(1)} \cdot \mathbf{R}_i^{(2)} = 0$ and $\|\mathbf{R}_i^{(1),(2)}\| = 1$ — equations required for $\mathbf{R}_i \in \text{SO}(3)$. Observe that (16a)-(16c) also fix the trace of \mathbf{Y}_i . The matrix \mathbf{Y}_i contains also all the elements of the third column through $\mathbf{R}_i^{(3)} = \mathbf{R}_i^{(1)} \times \mathbf{R}_i^{(2)}$.

We can represent all three columns of \mathbf{R}_i using a linear mapping $g(\cdot) := \mathbb{R}^{7 \times 7} \rightarrow \mathbb{R}^{3 \times 3}$, $\mathbf{R}_i = g(\mathbf{Y}_i)$; this map $g(\cdot)$ does not guarantee the rotation constraint $\mathbf{R}_i \in \text{SO}(3)$ unless accompanied by additional constraints:

Theorem 1: A matrix $\mathbf{R}_i = g(\mathbf{Y}_i)$ is a rotation matrix (i.e., $\mathbf{R}_i \in \text{SO}(3)$) if and only if $\mathbf{Y}_i \in \mathcal{Y}$ and $\text{rank}(\mathbf{Y}_i) = 1$.

See [23] for a proof.

Theorem 1 shows that our relaxation of $\text{SO}(3)$ is tight on the rank-1 set, meaning that we can solve for a solution on the relaxed set and exactly recover the corresponding rotations.

B. Relaxation of a subset of $\mathbb{R} \times \mathcal{S}^2$

Consider a space of unit vectors $\mathbf{v} \in \mathcal{S}^2$ and a set of real numbers $\tau \in [0, 1]$. The tuple (τ, \mathbf{v}) forms a subset of $\mathbb{R} \times \mathcal{S}^2$ (in many applications, this can be the distance and direction of a 3-D vector). We now introduce a way to formulate variables in this subset as fixed-trace matrices, similar to what is done for rotations in Section IV-A.

Definition 2: Given $\tau \in [0, 1]$ and $\mathbf{v} = [v_1 \ v_2 \ v_3]^\top \in \mathbb{R}^3$, define three matrices $\{\mathbf{Y}_{\tau,l}\}_3$ as:

$$\mathbf{Y}_{\tau,l} = \begin{bmatrix} \sqrt{\tau}v_l \\ \sqrt{1-\tau}v_l \\ \sqrt{\tau} \\ \sqrt{1-\tau} \end{bmatrix} \begin{bmatrix} \sqrt{\tau}v_l \\ \sqrt{1-\tau}v_l \\ \sqrt{\tau} \\ \sqrt{1-\tau} \end{bmatrix}^\top, \quad l \in \{1, 2, 3\}, \quad (17)$$

and define the constraint $\{\mathbf{Y}_{\tau,l}\}_3 \in \mathcal{Y}_\tau$ as:

- 1) $\mathbf{Y}_{\tau,l} \succeq 0$;
- 2) $\sum_{l=1}^3 \text{tr}(\mathbf{Y}_{\tau,l}) = 4$;
- 3) $\mathbf{Y}_{\tau,l}(3, 3) + \mathbf{Y}_{\tau,l}(4, 4) = 1$;
- 4) $\mathbf{Y}_{\tau,l}(1, 4) = \mathbf{Y}_{\tau,l}(2, 3)$;
- 5) $\mathbf{Y}_{\tau,l}(1, 3), \mathbf{Y}_{\tau,l}(1, 4), \mathbf{Y}_{\tau,l}(2, 3), \mathbf{Y}_{\tau,l}(2, 4) \in [-1, 1]$;
- 6) $\mathbf{Y}_{\tau,l}(3, 3) \in [0, 1]$, $\mathbf{Y}_{\tau,l}(3, 4) \in [0, 1]$;
- 7) $\mathbf{Y}_{\tau,l}(3, 3) = \mathbf{Y}_{\tau,l'}(3, 3)$, $\mathbf{Y}_{\tau,l}(3, 4) = \mathbf{Y}_{\tau,l'}(3, 4)$;
- 8) $\sum_{l=1}^3 \mathbf{Y}_{\tau,l}(1, 2) = \mathbf{Y}_{\tau,1}(3, 4)$;
- 9) $\sum_{l=1}^3 \mathbf{Y}_{\tau,l}(1, 1) = \mathbf{Y}_{\tau,1}(3, 3)$, $\sum_{l'=1}^3 \mathbf{Y}_{\tau,l'}(2, 2) = \mathbf{Y}_{\tau,1}(4, 4)$;

unless appearing in a sum, the constraints should hold for all $l, l' \in \{1, 2, 3\}$, $l \neq l'$.

Definition 2 parallels [23], where the matrix is the outer product of $[\sqrt{\tau}\mathbf{v} \ \sqrt{1-\tau}\mathbf{v} \ \sqrt{\tau} \ \sqrt{1-\tau}]^\top$; however, $\{\mathbf{Y}_{\tau,l}\}_3$ is smaller (48 vs. 64 variables) by excluding unused cross-terms while retaining the necessary submatrices, with the role of the constraints \mathcal{Y}_τ explained below:

- Constraint 2) fixes the sum of traces of $\{\mathbf{Y}_{\tau,l}\}_3$ and 3) fixes the trace of each 2×2 diagonal submatrix.
- Constraint 4) restricts the off-diagonal equalities of each $\mathbf{Y}_{\tau,l}$ and 5) restricts the bounds of these elements.
- Constraint 6) restricts the joint position limit $\tau \in [0, 1]$.
- Constraint 7) enforces the consistency of τ and $\sqrt{\tau(1-\tau)}$ between any two $\mathbf{Y}_{\tau,l}$.
- Constraints 8) and 9) both involve a sum over elements across different $l \in \{1, 2, 3\}$ based on the fact that $\sum_l v_l^2 = 1$ when $\|\mathbf{v}\| = 1$.

The following theorem shows that $\tau \in [0, 1]$ and $\mathbf{v} \in \mathcal{S}^2$ can be recovered linearly from rank-1 \mathbf{Y}_τ .

Theorem 2: Define the following function $g_\tau : \mathbb{R}^{4 \times 4 \times 3} \rightarrow \mathbb{R} \times \mathcal{S}^2$.

$$\begin{aligned} (\tau, \mathbf{v}) &= g_\tau(\{\mathbf{Y}_{\tau,l}\}_3) \\ &:= (\mathbf{Y}_{\tau,1}(3, 3), \text{stack}\{\mathbf{Y}_{\tau,l}(1, 3) + \mathbf{Y}_{\tau,l}(2, 4)\}_3) \end{aligned} \quad (18)$$

Let $(\tau, \mathbf{v}) := g_\tau(\{\mathbf{Y}_{\tau,l}\}_3)$. When the matrices $\{\mathbf{Y}_{\tau,l}\}_3 \in \mathcal{Y}_\tau$ and $\text{rank}(\mathbf{Y}_{\tau,l}) = 1, \forall l$, it holds that

$$\tau \in [0, 1], \text{ and } \|\mathbf{v}\| = 1 \quad (19)$$

Proof: By (6)), $\tau \in [0, 1]$ holds at rank-1 \mathbf{Y}_τ^k . When each matrix $\mathbf{Y}_{\tau,l}$ is rank-1, it can be written as

$$\mathbf{Y}_{\tau,l} = \hat{\mathbf{y}}\hat{\mathbf{y}}^\top \quad (20)$$

where $\hat{\mathbf{y}} = [s_1\sqrt{a_l} \ s_2\sqrt{b_l} \ s_3\sqrt{c_l} \ s_4\sqrt{d_l}]^\top$, and s_1, \dots, s_4 are sign indicator ± 1 . Then the l.h.s. of (19) equals to

$$\sum_{l=1}^3 a_l c_l + b_l d_l + 2s_1 s_2 s_3 s_4 \sqrt{a_l b_l c_l d_l} \quad (21)$$

Based on constraints 3) and 7), we let $\hat{\tau} = c_l, \forall l$ and we have $d_l = 1 - \hat{\tau}, \forall l$. By constraint 9) we have $\sum_{l=1}^3 a_l = \hat{\tau}$ and $\sum_{l=1}^3 b_l = 1 - \hat{\tau}$. By constraint 8) we have $s_1 s_2 \sum_{l=1}^3 \sqrt{a_l b_l} = s_3 s_4 \sqrt{c_l d_l} = s_3 s_4 \hat{\tau}(1 - \hat{\tau})$. With these, (21) becomes

$$\hat{\tau}^2 + (1 - \hat{\tau})^2 + 2\hat{\tau}(1 - \hat{\tau}) = 1 \quad (22)$$

■

The following proposition shows that when $\{\mathbf{Y}_{\tau,l}\}_3$ is rank-one, the bilinear term $\tau\mathbf{v}$ can be recovered as a linear function of \mathbf{Y}_τ , ensuring the validity of the product.

Proposition 2: Define the function $g_{\tau v} : \mathbb{R}^{4 \times 4 \times 3} \rightarrow \mathbb{R}^3$.

$$g_{\tau v}(\{\mathbf{Y}_{\tau,l}\}_3) := \text{stack}\{\mathbf{Y}_{\tau,l}(1, 3)\}_3 \quad (23)$$

Let $(\tau, \mathbf{v}) := g_\tau(\{\mathbf{Y}_{\tau,l}\}_3)$. When the matrices $\{\mathbf{Y}_{\tau,l}\}_3 \in \mathcal{Y}_\tau$ and $\text{rank}(\mathbf{Y}_{\tau,l}) = 1, \forall l$, it holds that

$$g_{\tau v}(\{\mathbf{Y}_{\tau,l}\}_3) = \tau \mathbf{v} \quad (24)$$

Proof: We write $\mathbf{Y}_{\tau,l}$ in the form of (21) and proving (24) is equivalent to prove the following equality,

$$s_1 s_3 \sqrt{a_l c_l} = s_1 s_3 c_l \sqrt{a_l c_l} + s_2 s_4 c_l \sqrt{b_l d_l}, \quad \forall l = 1, \dots, 3 \quad (25)$$

By constraint 4) we have $s_2 s_3 \sqrt{b_l c_l} = s_1 s_4 \sqrt{a_l d_l}$. Substitute to the r.h.s of (25) to get $s_1 \sqrt{a_l c_l} (s_3 c_l + s_4 d_l)$. By constraints 6) and 3) we have $s_3 = s_4$ and $c_l + d_l = 1$. Substitute to (25) and the equality is proved. ■

We demonstrate in the following proposition that the rank-1 condition (5) can be obtained for every matrix in $\{\mathbf{Y}_{\tau,l}\}_3$ through maximization of a sum of $\lambda_1(\mathbf{Y}_{\tau,l})$.

Proposition 3: When $\sum_i \lambda_1(\mathbf{Y}_{\tau,l})$ is maximized and $\{\mathbf{Y}_{\tau,l}\}_3 \in \mathcal{Y}_\tau$, i.e.,

$$\{\mathbf{Y}_{\tau,l}^*\}_3 = \text{argmax}_l (\sum_i \lambda_1(\mathbf{Y}_{\tau,l})) \in \mathcal{Y}_\tau, \quad (26)$$

we have $\text{rank}(\mathbf{Y}_{\tau,l}^*) = 1, \forall l$.

Proof: Because the trace is also the sum of the eigenvalues, with the sum of the trace fixed, we have

$$\sum_{l=1}^3 \lambda_1(\mathbf{Y}_{\tau,l}) + \sum_{l=1}^3 \sum_{i=2}^4 \lambda_i(\mathbf{Y}_{\tau,l}) = 4. \quad (27)$$

Since the matrices are PSD, when $\{\mathbf{Y}_{\tau,l}^*\}_3 = \text{argmax}_l (\sum_i \lambda_1(\mathbf{Y}_{\tau,l}))$ we have $\sum_{l=1}^3 \sum_{i=2}^4 \lambda_i(\mathbf{Y}_{\tau,l}^*) = 0$. Thus $\text{rank}(\mathbf{Y}_{\tau,l}^*) = 1, \forall l \in \{1, 2, 3\}$. ■

V. Applications

In this section, we address three robotic problems via virtual robots, introducing the SP robot as a module for building virtual kinematic chains and showing that solutions on these chains correspond to solutions of the original problems.

A. Rigid translation using forward kinematics of a virtual kinematic chain

We start with the definition of a robot with two joints.

Definition 3: An SP robot has a spherical joint followed by a prismatic joint. The spherical joint centers at the base, and the prismatic joint has an extension limit of $[0, \tau_u]$. The end-effector is the free end of the prismatic joint.

Figure 2 visualizes an SP robot. The translation of the end-effector relative to the base is a function $p : \mathbb{R}^3 \times \mathbb{R} \times \mathbb{R}^3 \rightarrow \mathbb{R}^3$ defined as

$$p(\mathbf{t}, \tau, \mathbf{v}) = \mathbf{t} + \tau_u \tau \mathbf{v} \quad (28)$$

where \mathbf{v} is a unit vector aligned with the axis of the prismatic joint, and $\tau \in [0, 1]$ is the normalized prismatic joint position. We refer to (τ_i, \mathbf{v}_i) as the pose of the SP robot.

In the context of this paper, SP robots are a useful modeling tool because of the following property.

Lemma 1: Any rigid translation ${}^w \mathbf{t}_{b_2}$ can be represented using the forward kinematics of an SP robot based at b_1 , i.e.,

$${}^w \mathbf{t}_{b_2} = p({}^w \mathbf{t}_{b_1}, \tau, \mathbf{v}), \quad (29)$$

where \mathbf{v} is the unit vector aligned with the line connecting the origins of b_1 and b_2 , assuming the robot's extension cap $\tau_u \geq \|{}^w \mathbf{t}_{b_2} - {}^w \mathbf{t}_{b_1}\|$.

Proof: The unit vector is given by $\mathbf{v} = \frac{{}^w \mathbf{t}_{b_2} - {}^w \mathbf{t}_{b_1}}{\|{}^w \mathbf{t}_{b_2} - {}^w \mathbf{t}_{b_1}\|}$. Choose $\tau = \|{}^w \mathbf{t}_{b_2} - {}^w \mathbf{t}_{b_1}\|/\tau_u$ and (29) holds as long as $\tau_u \geq \|{}^w \mathbf{t}_{b_2} - {}^w \mathbf{t}_{b_1}\|$ (the prismatic joint is long enough). ■

As shown in Section IV-B, the variables $(\tau, \mathbf{v}) \in \mathbb{R} \times \mathcal{S}^2$ can be expressed as linear functions of \mathbf{Y}_τ , so any linear kinematic constraints on (τ, \mathbf{v}) remain linear in \mathbf{Y}_τ , enabling convex formulations of lifted variables from convex kinematics of a virtual robot.

B. Perspective-n-Point problem

We review the perspective-n-point (PnP) problem defined below.

Definition 4: Given the global coordinates of a set of points $\{\mathbf{q}_1, \dots, \mathbf{q}_n\}$ and their projections $\{\mathbf{p}_1, \dots, \mathbf{p}_n\}$ (in pixels) onto the image plane of a camera¹ with the intrinsic matrix \mathbf{K} , the PnP problem is to find the camera pose (\mathbf{R}, \mathbf{t}) such that

$$\tilde{\mathbf{p}}_i = \mathbf{K}(\mathbf{R}^\top \mathbf{q}_i - \mathbf{R}^\top \mathbf{t}), \quad \forall i = 1, \dots, n, \quad (30)$$

where $\tilde{\mathbf{p}}_i \in \mathbb{R}^3$ projects to the image coordinates \mathbf{p}_i , i.e., $\mathbf{p}_i = [\tilde{\mathbf{p}}_i^{(1)}/\tilde{\mathbf{p}}_i^{(3)} \quad \tilde{\mathbf{p}}_i^{(2)}/\tilde{\mathbf{p}}_i^{(3)}]^\top$. We define $\hat{\mathbf{p}}_i$ as a unit vector from the camera origin passing \mathbf{p}_i .

We define the following associated optimization problem.

Problem 6 (PnP Problem):

$$\min_{\mathbf{R} \in \text{SO}(3), \mathbf{t} \in \mathbb{R}^3, \{\tau_i\}_n \in \mathbb{R}^n} \sum_i^n \left\| \frac{\mathbf{q}_i - \mathbf{t}}{\tau_i} - \mathbf{R} \hat{\mathbf{p}}_i \right\|_2^2 \quad (31)$$

The factor τ_i is a positive scalar. The vector $\hat{\mathbf{p}}_i$ is obtained by normalizing $[\mathbf{p}_i \quad f_{cam}]^\top$, where f_{cam} is the camera focal length.

We introduce the following proposition to show that solving Problem 6 is equivalent to solving Definition 4.

Proposition 4: A pose $(\mathbf{R}^*, \mathbf{t}^*)$ is a solution to the PnP problem in Definition 4 if and only if there exists a $\{\tau_i^*\}_n$ such that $(\mathbf{R}^*, \mathbf{t}^*, \{\tau_i^*\}_n)$ is a minimizer of Problem 6, and the corresponding minimal cost is zero.

Proof: On the one hand, a minimizer $(\mathbf{R}^*, \mathbf{t}^*, \{\tau_i^*\}_n)$ of Problem 6 yields the relation

$$\mathbf{q}_i - \mathbf{t}^* = \tau_i^* \mathbf{R}^* \hat{\mathbf{p}}_i. \quad (32)$$

We substitute (32) along with $\mathbf{K} = \text{diag}(f_{cam}, f_{cam}, 1)$ and $\hat{\mathbf{p}}_i = [\mathbf{p}_i \quad f_{cam}]^\top / (\|\mathbf{p}_i\|)$ to the r.h.s. of (30):

$$r.h.s. = \tau_i^* f_{cam} / (\|\mathbf{p}_i\|) [\mathbf{p}_i \quad 1]^\top. \quad (33)$$

¹Throughout this work, we assume the camera has no distortion and the principal points are located at $(0, 0)$ of the image plane [7], [11].

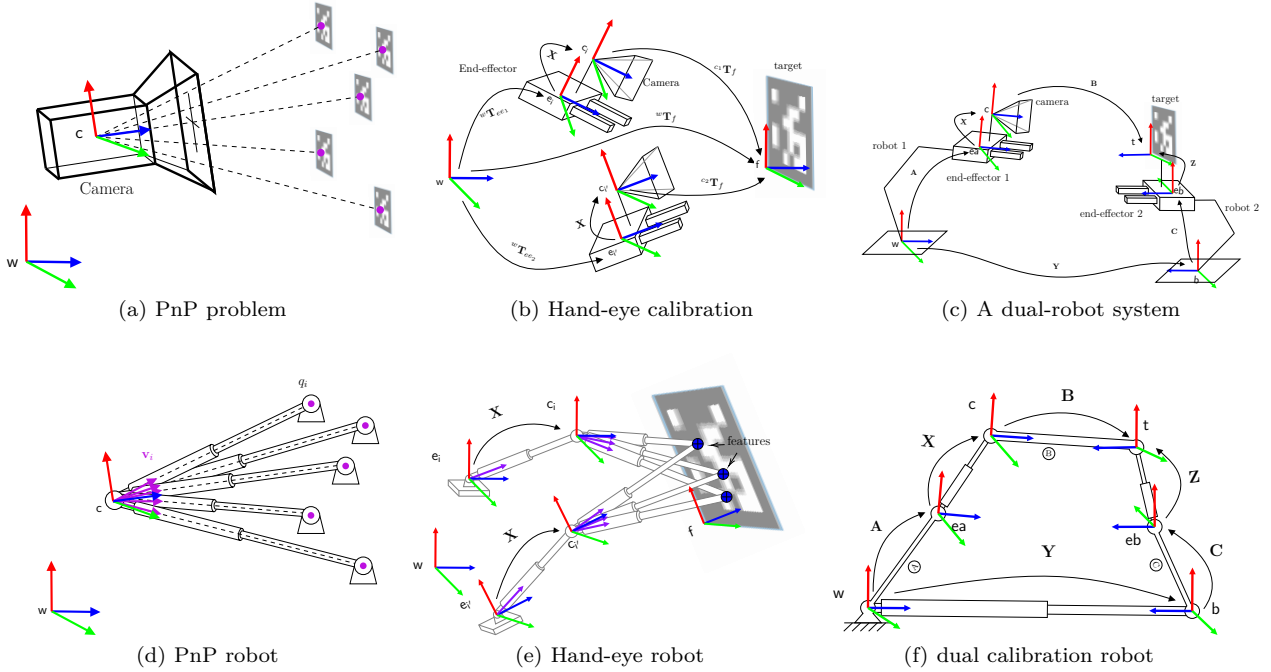


Fig. 1: Some estimation and calibration problems in robotics can be formulated as kinematics problems of virtual robots.

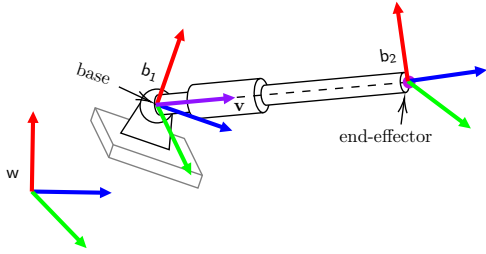


Fig. 2: For any two reference frames b_1 and b_2 , the rigid translation ${}^w\mathbf{t}_{b_2}$ can be represented using the forward kinematics of an SP robot.

It can be seen that \mathbf{p}_i can be recovered by dividing (33) by the third entry of itself, thus matching Definition 4.

On the other hand, because \mathbf{p}_i is the projection of \mathbf{q}_i onto the image plane, $\mathbf{q}_i - \mathbf{t}$ and $\mathbf{R}\mathbf{p}_i$ are collinear. Moreover, because $\hat{\mathbf{p}}_i$ is a normalization of \mathbf{p}_i , $\mathbf{q}_i - \mathbf{t}$ and $\mathbf{R}\hat{\mathbf{p}}_i$ are collinear. Therefore there exists factors $\{\tau_i\}_n$ such that $\frac{\mathbf{q}_i - \mathbf{t}}{\tau_i} = \mathbf{R}\hat{\mathbf{p}}_i, \forall i = 1, \dots, n$ and $(\mathbf{R}, \mathbf{t}, \{\tau_i\}_n)$ is a minimizer of Problem 6. ■

Assumption 1: The following conditions hold true:

- 1) $n \geq 6$;
- 2) The points \mathbf{q}_i are in general position, meaning four or more of them do not lie on a single plane in \mathbb{R}^3 ;

We then have the following regarding the uniqueness of the solution of the PnP problem.

Lemma 2 ([5]): When Assumption 1 holds, the PnP problem in Definition 4 has a unique solution.

We define the following assembly of SP robots.

Definition 5: A PnP robot is comprised of n SP robots with poses (τ_i, \mathbf{v}_i) , where all of their spherical joints share

the same parent, which we call the base. We denote the pose of the base $({}^w\tilde{\mathbf{R}}_c, {}^w\tilde{\mathbf{t}}_c)$.

C. Hand-eye calibration

The robot hand-eye calibration problem is the problem of finding the transformation between the robot end effector and a rigidly mounted camera². Suppose an object with an unknown pose $(\mathbf{R}_f, \mathbf{t}_f)$ is represented by n features and measured by the camera from multiple robot configurations indexed $i \in \{1, \dots, m\}$. We denote \mathbf{e}_i and \mathbf{c}_i as the frames of the end-effector and the camera under robot configuration i , respectively. Consider any two configurations i and i' as shown in Fig. 1b, the hand-eye calibration problem can be formulated using the following relation

$$\mathbf{AX} = \mathbf{XB} \quad (34)$$

where

$$\begin{aligned} \mathbf{A} &= ({}^w\mathbf{T}_{e_{i'}})^{-1} {}^w\mathbf{T}_{e_i}, \text{ and} \\ \mathbf{B} &= c_{i'} \mathbf{T}_f (c_i \mathbf{T}_f)^{-1}. \end{aligned} \quad (35)$$

Transformations ${}^w\mathbf{T}_{e_2}, {}^w\mathbf{T}_{e_1}$ are computed by performing robot calibration and ${}^{c_2}\mathbf{T}_f, {}^{c_1}\mathbf{T}_f$ are found from camera calibration. The goal of hand-eye calibration is to find the unknown transformation matrix \mathbf{X} as a solution to (34). The transformation \mathbf{X} can be decomposed into $\mathbf{R}_x \in \text{SO}(3)$ and $\mathbf{t}_x \in \mathbb{R}^3$.

We define a virtual robot for the hand-eye calibration task by combining SP and PnP robots.

²In this paper, we consider the eye-in-hand calibration, meaning that the camera is fixed on the end-effector of the robot.

Definition 6: A hand-eye robot has m bases, where the transformation from each base $i \in \{1, \dots, m\}$ to the world is ${}^w\mathbf{T}_{e_i}$. From each base, an SP robot connects to the camera origin of \mathbf{c}_i . A PnP robot connects to all features $\{f_j\}_n$ and the base of the PnP robot is attached to \mathbf{c}_i . We denote the sets of all poses of the hand-eye robot as $(\boldsymbol{\tau}, \mathcal{V})$.

A visualization of the hand-eye robot is in Fig. 1e.

D. Simultaneous calibration of dual-robot systems

We consider another calibration scenario shown in Fig. 1c, where the hand-eye, hand-target, and robot-robot transformations are calibrated simultaneously. The coordinate systems \mathbf{ea} , \mathbf{eb} , \mathbf{c} , \mathbf{t} , and \mathbf{b} are rigidly attached to the end-effector of robot 1, the end-effector of robot 2, the camera attached to robot 1, the calibration target attached to robot 2, and the base of robot 2, respectively. The relations among these coordinate systems satisfy the equation

$$\mathbf{AXB} = \mathbf{YCZ}, \quad (36)$$

where \mathbf{X} , \mathbf{Y} , and \mathbf{Z} are the unknown transformation matrices

$$\mathbf{X} = \mathbf{T}_{ea}^{-1} \mathbf{T}_c, \quad \mathbf{Y} = \mathbf{T}_b, \quad \mathbf{Z} = \mathbf{T}_{eb}^{-1} \mathbf{T}_t. \quad (37)$$

The matrices \mathbf{A} , \mathbf{B} , and \mathbf{C} are the measured transformations

$$\mathbf{A} = {}^w\mathbf{T}_{ea}, \quad \mathbf{B} = {}^c\mathbf{T}_t, \quad \mathbf{C} = {}^b\mathbf{T}_{eb}. \quad (38)$$

We propose the following virtual robot for the simultaneous calibration of dual-robot systems.

Definition 7: A dual calibration robot has three fixed links, parts (A), (B), and (C). Reference frames are attached to the ends of the three parts. The transformation between the two attached reference frames are fixed to the values \mathbf{A} , \mathbf{B} , and \mathbf{C} for (A), (B), and (C), respectively. Each pair of the parts is connected via a spherical joint followed by a prismatic joint, then another spherical joint, as shown in Figure 1f. The lower end of (A) is rigidly attached to the world reference frame. The dual-robot system may have different configurations, where m measurements $\{\mathbf{A}_i, \mathbf{B}_i, \mathbf{C}_i\}_m$ are taken.

The coordinate systems in the dual-robot system can be represented by the reference frames of a dual calibration robot. The parameters \mathbf{A} , \mathbf{B} , and \mathbf{C} are modeled using rigid bodies, while the unknown transformations \mathbf{X} , \mathbf{Y} , and \mathbf{Z} are represented using SP robots. The unknown transformations \mathbf{X} , \mathbf{Y} , \mathbf{Z} are assumed to remain the same among different configurations, i.e.,

$$\mathbf{X}_i = \mathbf{X}_{i'}, \mathbf{Z}_i = \mathbf{Z}_{i'}, \text{ and } \mathbf{Y}_i = \mathbf{Y}_{i'}, \quad \forall i, i' = 1, \dots, m. \quad (39)$$

Such equality of transformations will be discussed in detail in Section V-E.

Problem	PnP	Hand-Eye	Dual Calibration
Number of SP robots	n	$m(n+1)$	$3m$
Number of unknown Rotations	1	$m+1$	$3m$
Objective Function f_k	Reproj. Error	Reproj. Error	$\ \mathbf{AXB} - \mathbf{YCZ}\ _F$
Constraints	Kine. Closure	Kine. Closure, \mathbf{X} Equality	$\mathbf{X}, \mathbf{Y}, \mathbf{Z}$ Equality

TABLE II: Kinematics problems of the virtual robots

E. Kinematics problems

We define the following kinematics problem for the PnP, hand-eye, and dual calibration robots. See Table II for a summary of the problem settings for specific problems.

Problem 7 (Kinematics Problem of Virtual Robots):

$$\min_{\boldsymbol{\tau}, \mathcal{V}, \mathcal{R}} f_k(\boldsymbol{\tau}, \mathcal{V}, \mathcal{R}) \quad (40a)$$

$$\text{s.t.} \quad e_{kc}(\boldsymbol{\tau}, \mathcal{V}, \mathcal{R}) = 0 \quad (40b)$$

$$e_{te}(\boldsymbol{\tau}, \mathcal{V}, \mathcal{R}) = 0 \quad (40c)$$

The variable $\{\boldsymbol{\tau}, \mathcal{V}\}$ is the set of poses of SP robots. The variable \mathcal{R} is the set of unknown rotation matrices. The functions f_k , e_{kc} and e_{te} stand for the kinematics objective, kinematic closure and transformation equality functions, respectively, which we discuss in detail below with example.

Objective function. The objective functions encode the estimation and calibration metrics. For the PnP and hand-eye robots, the objective is the reprojection error, defined as the norm of the difference between the prismatic joint unit vectors \mathbf{v}_i and the oriented measurements $\mathbf{R}_c \hat{\mathbf{p}}_i$. For the dual calibration robot, the objective is given by $\|\mathbf{AXB} - \mathbf{YCZ}\|_F$.

Constraints. The kinematic constraints of the following types are defined to restrict the feasible set so that any solution to the kinematics problem is also a feasible solution to the original estimation or calibration problem.

- Kinematic closure. This constraint restricts the kinematic closure of the kinematic chains.
- Transformation Equality. This constraint restricts the consistency of some transformations in different configurations. For example, $\mathbf{X}_i = \mathbf{X}_{i'}$ for any two measurements $i \neq i'$.

Example 1 (PnP robot kinematics): The following proposition relates the kinematics problems of the PnP robot and the PnP problem.

Proposition 5: Let $\{\mathbf{q}_1, \dots, \mathbf{q}_n\}$ be a set of points in general positions and $n \geq 6$, and let $\{\mathbf{p}_1, \dots, \mathbf{p}_n\}$ be their projections onto the image plane of a camera with intrinsics \mathbf{K} and pose $({}^w\mathbf{R}_c, {}^w\mathbf{t}_c)$. We attach every end-effector of a PnP robot to \mathbf{q}_i . Then $({}^w\mathbf{R}_c, {}^w\tilde{\mathbf{t}}_c) = ({}^w\mathbf{R}_c, {}^w\mathbf{t}_c)$ if and only if $(\{\mathbf{v}_i, \tau_i\}_n, {}^w\tilde{\mathbf{R}}_c, {}^w\tilde{\mathbf{t}}_c)$ is a minimizer of

Problem 8 (PnP Robot Kinematics):

$$\min_{\{\mathbf{v}_i, \tau_i\}_n, {}^w\tilde{\mathbf{R}}_c, {}^w\tilde{\mathbf{t}}_c} f_k := \sum_i^n \|\mathbf{v}_i - {}^w\tilde{\mathbf{R}}_c \hat{\mathbf{p}}_i\|_2^2 \quad (41a)$$

$$\text{s.t. } p({}^w\tilde{\mathbf{t}}_c, \tau_i, \mathbf{v}_i) = \mathbf{q}_i, \forall i = 1, \dots, n \quad (41b)$$

and the corresponding minimal cost is zero.

Proof: On the one hand, when $(\{\mathbf{v}_i, \tau_i\}_n, {}^w\tilde{\mathbf{R}}_c, {}^w\tilde{\mathbf{t}}_c)$ minimizes the objective function and the corresponding cost is zero, we have $\mathbf{v}_i = {}^w\tilde{\mathbf{R}}_c \hat{\mathbf{p}}_i$ and ${}^w\tilde{\mathbf{t}}_c + \tau_i \mathbf{v}_i = \mathbf{q}_i, \forall i = 1, \dots, n$. This means that $\frac{\mathbf{q}_i - {}^w\tilde{\mathbf{t}}_c}{\tau_i} = {}^w\tilde{\mathbf{R}}_c \hat{\mathbf{p}}_i$. By Proposition 4, we know that $({}^w\tilde{\mathbf{R}}_c, {}^w\tilde{\mathbf{t}}_c)$ is a solution to the PnP problem and therefore $({}^w\tilde{\mathbf{R}}_c, {}^w\tilde{\mathbf{t}}_c) = ({}^w\mathbf{R}_c, {}^w\mathbf{t}_c)$.

On the other hand, when $({}^w\tilde{\mathbf{R}}_c, {}^w\tilde{\mathbf{t}}_c) = ({}^w\mathbf{R}_c, {}^w\mathbf{t}_c)$, by Proposition 4, there exists a $\{\tilde{\tau}_i\}_n$ such that $\frac{\mathbf{q}_i - {}^w\tilde{\mathbf{t}}_c}{\tilde{\tau}_i} = {}^w\tilde{\mathbf{R}}_c \hat{\mathbf{p}}_i, \forall i = 1, \dots, n$. Let $\tilde{\tau}_i = \tau_i \tilde{\tau}_i$ and $\mathbf{v}_i = \frac{\mathbf{q}_i - {}^w\tilde{\mathbf{t}}_c}{\tilde{\tau}_i}$ and $(\{\mathbf{v}_i, \tau_i\}_n, {}^w\tilde{\mathbf{R}}_c, {}^w\tilde{\mathbf{t}}_c)$ is a minimizer of Problem 8 with minimal cost equals to zero. ■

Problem 8 minimizes the reprojection error (41a) while constraining the kinematic closure through (41b). Proposition 5 enables us to convert a PnP problem to a kinematics problem of a virtual PnP robot.

Example 2 (Hand-eye robot Kinematic constraints): We investigate the hand-eye robot to demonstrate the kinematics constraints. Observe that (34) is equivalent to the following equation by substituting (35)

$${}^w\mathbf{T}_{e_i} \mathbf{X}^{c_i} \mathbf{T}_f = {}^w\mathbf{T}_{e_{i'}} \mathbf{X}^{c_{i'}} \mathbf{T}_f \quad (42)$$

It can be seen that (42) encodes two constraints $\forall i, i' \in \{1, \dots, m\}$:

$$\text{Kinematics closure: } {}^w\mathbf{T}_{e_i} {}^{e_i} \mathbf{T}_{c_i} {}^{c_i} \mathbf{T}_f = {}^w\mathbf{T}_{e_{i'}} {}^{e_{i'}} \mathbf{T}_{c_{i'}} {}^{c_{i'}} \mathbf{T}_f \quad (43a)$$

$$\text{Transformation equality: } \mathbf{X} = {}^{e_i} \mathbf{T}_{c_i} = {}^{e_{i'}} \mathbf{T}_{c_{i'}}. \quad (43b)$$

The (43a) is a kinematic closure constraint, meaning that the transformations from the target to the world frame are the same following the kinematic chain of every measurement: $f \rightarrow c_i \rightarrow e_i$. Constraint (43b) enforces that the transformations $\{{}^{e_i} \mathbf{T}_{c_i}\}_m$ equals \mathbf{X} for every measurement.

F. Semi-Definite Relaxation

Consider the variable set

$$\mathcal{X} := \{\boldsymbol{\tau}, \mathcal{V}, \mathcal{R}, \boldsymbol{\tau}\mathcal{V}\} \quad (44)$$

The set $\boldsymbol{\tau}\mathcal{V}$ is the product set $\boldsymbol{\tau}\mathcal{V} := \{\boldsymbol{\tau}\mathbf{v} \mid \boldsymbol{\tau} \in \boldsymbol{\tau}, \mathbf{v} \in \mathcal{V}\}$. In general, for the defined virtual robots, the kinematics Problem 7 consists of (i) an objective function f_k that is quadratic to \mathcal{X} , and (ii) constraints linear to \mathcal{X} . This means Problem 7 is convex in \mathcal{X} (see Problem 8 for an example).

As we have shown in Section IV-A and IV-B, \mathcal{R} , and $\boldsymbol{\tau}, \mathcal{V}, \boldsymbol{\tau}\mathcal{V}$ can be represented exactly using rank-1 matrices $\mathbf{Y} = \{\mathbf{Y}_i \mid \mathbf{Y}_i \in \mathcal{Y}\}$, $\mathbf{Y}_\tau = \{\{\mathbf{Y}_\tau\}_3 \mid \{\mathbf{Y}_\tau\}_3 \in \mathcal{Y}_\tau\}$ through linear functions $g(\mathbf{Y})$, $g_\tau(\mathbf{Y}_\tau)$, and $g_{\tau\mathcal{V}}(\mathbf{Y}_\tau)$. Using this, we propose Algorithm 1 for solving \mathcal{X} .

Remark 1: We remark that, for the dual hand-eye robot, \mathcal{X} needs to include $\mathcal{V}\mathcal{R}, \mathcal{R}\mathcal{R}$ for Problem 7 to be convex. We will discuss how to account for these additional variables in Section VI-D.

Algorithm 1 Solution procedure for Problem 7

- 1: Develop Problem 1 from Problem 7 by representing \mathcal{X} using linear functions of $\mathbf{Y}, \mathbf{Y}_\tau$.
- 2: Solve Problem 1 to obtain an initial feasible solution $(\mathbf{Y}^0, \mathbf{Y}_\tau^0)$ not necessarily rank-1.
- 3: Move $(\mathbf{Y}^0, \mathbf{Y}_\tau^0)$ to a rank-1 solution $(\mathbf{Y}^r, \mathbf{Y}_\tau^r)$ by iteratively solving Problem 4.
- 4: Move $(\mathbf{Y}^r, \mathbf{Y}_\tau^r)$ by iteratively solving sequences of Problem 5 to a low-cost solution $(\hat{\mathbf{Y}}, \hat{\mathbf{Y}}_\tau)$ up to a tolerance ϵ , i.e., $f(\hat{\mathbf{Y}}, \hat{\mathbf{Y}}_\tau) < \epsilon$.
- 5: Certify the optimality by solving the dual Problem 3 and checking the duality gap.

VI. Kinematics Problems of Virtual Robots

In this section, we first introduce a general formulation of the transformation equality constraint. Then, we investigate the kinematics problems of the hand-eye and dual calibration robots.

A. Constraint on constant transformation between two reference frames

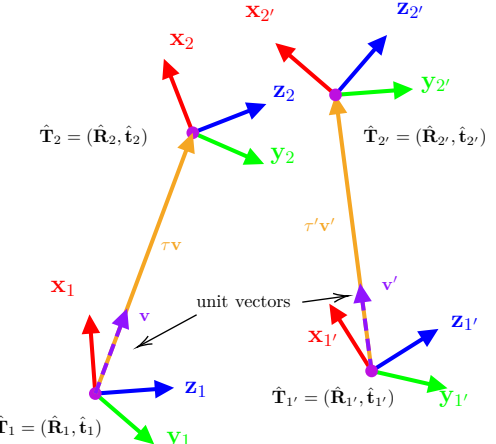


Fig. 3: The consistency of transformations between reference frames with unknown absolute poses, $\mathbf{T}_1^{-1} \mathbf{T}_2 = \mathbf{T}_{1'}^{-1} \mathbf{T}_{2'}$, can be enforced through constraints on $\hat{\mathbf{R}}_1, \hat{\mathbf{R}}_2, \hat{\mathbf{R}}_{1'}, \hat{\mathbf{R}}_{2'}$, τ, τ', \mathbf{v} , and \mathbf{v}' .

Consider two reference frames f_1, f_2 and their corresponding frames after some rigid-body transformations, f'_1, f'_2 . We denote the global poses $\hat{\mathbf{T}}_1 := {}^w\mathbf{T}_{f_1} = (\hat{\mathbf{R}}_1, \hat{\mathbf{t}}_1)$ and $\hat{\mathbf{T}}_2 := {}^w\mathbf{T}_{f_2} = (\hat{\mathbf{R}}_2, \hat{\mathbf{t}}_2)$ (and similarly, $\hat{\mathbf{T}}_{1'}, \hat{\mathbf{T}}_{2'}$). Suppose the two frames are attached rigidly and the relative transformation remains the same, i.e., ${}^{f_1} \mathbf{T}_{f_2} = {}^{f_1'} \mathbf{T}_{f_2'}$, which is equivalent to

$$\hat{\mathbf{T}}_1^{-1} \hat{\mathbf{T}}_2 = \hat{\mathbf{T}}_{1'}^{-1} \hat{\mathbf{T}}_{2'}. \quad (45)$$

The decoupled translations and rotations of (45) satisfy

$$\hat{\mathbf{R}}_1^\top (\hat{\mathbf{t}}_2 - \hat{\mathbf{t}}_1) = \hat{\mathbf{R}}_{1'}^\top (\hat{\mathbf{t}}_{2'} - \hat{\mathbf{t}}_{1'}) \quad (46a)$$

$$\hat{\mathbf{R}}_1^\top \hat{\mathbf{R}}_2 = \hat{\mathbf{R}}_{1'}^\top \hat{\mathbf{R}}_{2'}. \quad (46b)$$

Recall that, by Lemma 1, $\hat{\mathbf{t}}_2$ can be represented using the forward kinematics of an SP robot connecting the frames 1 and 2. We denote the prismatic variables of this SP robot as τ, \mathbf{v} and τ', \mathbf{v}' between the motion, then substitute $\hat{\mathbf{t}}_2 = p(\hat{\mathbf{t}}_1, \tau, \mathbf{v})$, $\hat{\mathbf{t}}_{2'} = p(\hat{\mathbf{t}}_1, \tau', \mathbf{v}')$ into the (46a) and get

$$\hat{\mathbf{R}}_1^\top \tau \mathbf{v} = \hat{\mathbf{R}}_1^\top \tau' \mathbf{v}'. \quad (47)$$

Definition 8: For two reference frame 1 and 2, the transformation equality constraint is defined as $\{\tau, \mathbf{v}, \hat{\mathbf{R}}_1, \hat{\mathbf{R}}_2, \tau', \mathbf{v}', \hat{\mathbf{R}}_{1'}, \hat{\mathbf{R}}_{2'}\} \in \mathcal{C}_{ft}$ such that

$$\tau = \tau'. \quad (48a)$$

$$\hat{\mathbf{R}}_1^{(l_1)\top} \mathbf{v} = \hat{\mathbf{R}}_{1'}^{(l_1)\top} \mathbf{v}', \forall l_1 = 1, 2, 3, \text{ and}, \quad (48b)$$

$$\hat{\mathbf{R}}_1^{(l_1)\top} \hat{\mathbf{R}}_2^{(l_2)} = \hat{\mathbf{R}}_{1'}^{(l_1)\top} \hat{\mathbf{R}}_{2'}^{(l_2)}, \forall l_1 \in \{1, 2, 3\}, l_2 \in \{1, 2\}. \quad (48c)$$

The indices $\{l_1, l_2\}$ are for the columns of the rotation matrices $\hat{\mathbf{R}}_1$ and $\hat{\mathbf{R}}_2$.

Proposition 6: The relative transformation between two reference frames 1 and 2 remains the same, i.e., (46) holds, if and only if $\{\tau, \mathbf{v}, \hat{\mathbf{R}}_1, \hat{\mathbf{R}}_2, \tau', \mathbf{v}', \hat{\mathbf{R}}_{1'}, \hat{\mathbf{R}}_{2'}\} \in \mathcal{C}_{ft}$.

Proof: We start with the relative translation (46a) by multiplying τ and τ' on left and right of (48b) and concatenate for all of the columns i we obtain $\hat{\mathbf{R}}_1^\top (\hat{\mathbf{t}}_2 - \hat{\mathbf{t}}_1) = \hat{\mathbf{R}}_{1'}^\top (\hat{\mathbf{t}}_{2'} - \hat{\mathbf{t}}_{1'})$.

We now prove for the relative rotation (46b). Rotation preserves cross product, meaning that

$$\hat{\mathbf{R}}_1^{(i)\top} (\hat{\mathbf{R}}_2^{(1)} \times \hat{\mathbf{R}}_2^{(2)}) = (\hat{\mathbf{R}}_1^{(i)\top} \hat{\mathbf{R}}_2^{(1)}) \times (\hat{\mathbf{R}}_1^{(i)\top} \hat{\mathbf{R}}_2^{(2)}). \quad (49)$$

Using this result and (48c), we can obtain

$$\hat{\mathbf{R}}_1^{(i)\top} (\hat{\mathbf{R}}_2^{(1)} \times \hat{\mathbf{R}}_2^{(2)}) = \hat{\mathbf{R}}_{1'}^{(i)\top} (\hat{\mathbf{R}}_{2'}^{(1)} \times \hat{\mathbf{R}}_{2'}^{(2)}), \forall i \in \{1, 2, 3\}. \quad (50)$$

Because $\hat{\mathbf{R}}_2^{(3)} = \hat{\mathbf{R}}_2^{(1)} \times \hat{\mathbf{R}}_2^{(2)}$, we have

$$\hat{\mathbf{R}}_1^{(i)\top} \hat{\mathbf{R}}_2^{(3)} = \hat{\mathbf{R}}_{1'}^{(i)\top} \hat{\mathbf{R}}_{2'}^{(3)}, \forall i \in \{1, 2, 3\}. \quad (51)$$

Then (46b) is a concatenation of (48c) and (51) for $(i, j) \in \{1, 2, 3\}$. \blacksquare

Intuitively, the reference frames are connected using SP robots, and the equality of the relative transformation can be bounded by (48) acting on the variables related to the SP robots.

Remark 2: For the dual calibration robot, the constraints (48b) and (48c) can be

- linear when \mathbf{R}_1 is known and \mathbf{R}_2 is unknown (e.g., \mathbf{X} and \mathbf{Y});
- quadratic when $\mathbf{R}_1, \mathbf{R}_2$ are both unknown (e.g., \mathbf{Z}).

For the latter case to fit in a convex problem, we will discuss how to relax these into linear constraints in Section VI-D.

B. Hand-eye robot

The hand-eye robot is designed to model the transformations within the hand-eye calibration problem using the robot's poses. Specifically, we have fixed the poses between the hand-eye robot's bases to be $\{{}^w\mathbf{T}_{e_i}\}_m$. Moreover, we want to represent the camera poses $\{{}^w\mathbf{T}_{c_i}\}_m$

using the pose of the PnP robots' bases $\{{}^w\tilde{\mathbf{R}}_{c_i}, {}^w\tilde{\mathbf{t}}_{c_i}\}_n$. Once these equivalences are established, we can find the solution to the hand-eye calibration problem \mathbf{X} by computing the relative transformation of the poses of \mathbf{e}_i and \mathbf{c}_i . We will show that this can be done using proper constraints.

To begin with, we define the unknown variables that, once solved in the kinematics problem, can be used to recover the transformation \mathbf{X} .

$$\{\mathbf{R}\} := \{\mathbf{R}_{c_i}\}_m, \mathbf{R}_f$$

$$\boldsymbol{\tau} := \{\tau_{e_i, c_i}\}_m, \{\tau_{c_i, f_j}\}_{i=1, \dots, m, j=1, \dots, n}, \text{ and} \quad (52)$$

$$\mathcal{V} := \{\mathbf{v}_{e_i, c_i}\}_m, \{\mathbf{v}_{c_i, f_j}\}_{i=1, \dots, m, j=1, \dots, n},$$

The rotations include all the camera orientations and the calibration object. The subscripts like $\{e_i, c_i\}$ mean that the prismatic variable is for the connection e_i and c_i . For brevity, we rename $\tau_{0i} := \tau_{e_i, c_i}$, $\mathbf{v}_{0i} := \mathbf{v}_{e_i, c_i}$, $\tau_{ij} := \tau_{c_i, f_j}$, and $\mathbf{v}_{ij} := \mathbf{v}_{c_i, f_j}$.

So far, we have derived the constraints in the form of (43). We first look at (43a), and define the forward kinematics of a chain: $\mathbf{e}_i \rightarrow \mathbf{c}_i \rightarrow f_j \rightarrow \mathbf{f}$.

$$p_{fk,ij}(\boldsymbol{\tau}, \mathcal{V}, {}^w\mathbf{R}_f) := p(p({}^w\mathbf{t}_{e_i}, \tau_{0i}, \mathbf{v}_{0i}), \tau_{ij}, \mathbf{v}_{ij}) - {}^w\mathbf{R}_f \mathbf{f}_j \quad (53)$$

The vector \mathbf{f}_j is the feature position relative to the feature frame, available before the calibration. Next, we equate (53) for different (i, j) to get

$$\begin{aligned} \forall i, i' = 1, \dots, m, \quad j, j' = 1, \dots, n : \\ p_{fk,ij}(\boldsymbol{\tau}, \mathcal{V}, {}^w\mathbf{R}_f) = p_{fk,i'j'}(\boldsymbol{\tau}, \mathcal{V}, {}^w\mathbf{R}_f) \end{aligned} \quad (54)$$

Observe that (54) is the translation part of (43a). We note that the rotation part for (43a) is trivial as the target

Next, we decouple (43b) into rotation and translation then substitute $\mathbf{t}_{c_i} = \mathbf{t}_{e_i} + \mathbf{R}_{e_i} \mathbf{e}_i \mathbf{t}_{c_i}$ and get

$$\mathbf{R}_{e_i}^\top \mathbf{R}_{c_i} = \mathbf{R}_{e_i'}^\top \mathbf{R}_{c_i} \quad (55a)$$

$$\mathbf{R}_{e_i}^\top \mathbf{t}_{c_i} - \mathbf{R}_{e_i'}^\top \mathbf{t}_{c_i} = \mathbf{R}_{e_i}^\top \mathbf{t}_{e_i} - \mathbf{R}_{e_i'}^\top \mathbf{t}_{e_i} \quad (55b)$$

Then we substitute $\mathbf{t}_{c_i} = p(\mathbf{t}_{e_i}, \tau_{0i}, \mathbf{v}_{0i})$ into (55b) and

$$\mathbf{R}_{e_i}^\top \tau_{0i} \mathbf{v}_{0i} = \mathbf{R}_{e_i'}^\top \tau_{0i'} \mathbf{v}_{0i'}. \quad (56)$$

Observe that (56) is exactly (47). Now, we summarize the objective function and constraints

$$h_k(\boldsymbol{\tau}, \mathcal{V}, \mathcal{R}) := f_1(\mathcal{V}, \mathbf{R}_{c_i}) = \sum_i^m \sum_j^n \|\mathbf{v}_{ij} - \mathbf{R}_{c_i} \hat{\mathbf{p}}_i\|_2^2 \quad (57)$$

$$e_{kc}(\boldsymbol{\tau}, \mathcal{V}, \mathcal{R}) = 0 : \quad (54)$$

$$e_{te}(\boldsymbol{\tau}, \mathcal{V}, \mathcal{R}) = 0 : \quad (55a), (56)$$

Proposition 7: When the features satisfy Assumption 1, if there exists a solution $(\boldsymbol{\tau}^*, \mathcal{V}^*, \mathbf{R}_{c_i}^*, \mathbf{R}_f^*)$ to Problem 7 using the setting (57) and $f_1(\mathcal{V}^*, \mathbf{R}_{c_i}^*) = 0$, then the camera poses $\{{}^w\hat{\mathbf{T}}_{c_i}\}_m := \{(\mathbf{R}_{c_i}^*, p(\mathbf{t}_{e_i}^*, \tau_{0i}^*, \mathbf{v}_{0i}^*))\}_m$ equals the camera poses $\{{}^w\mathbf{T}_{c_i}\}_m$ in the hand-eye calibration problem and $\mathbf{X} = {}^w\mathbf{T}_{e_i}^\top {}^w\mathbf{T}_{c_i}$.

Proof: By Proposition 5 we know that the camera pose ${}^w\hat{\mathbf{T}}_{c_i} = (\hat{\mathbf{R}}_{c_i}, \hat{\mathbf{t}}_{c_i})$ is unique for the measurement of each camera c_i . Thus ${}^w\hat{\mathbf{T}}_{c_i} = {}^w\mathbf{T}_{c_i}$ because otherwise the uniqueness would be violated. Because $\hat{\mathbf{t}}_{c_i}$ is fixed, the SP robot between e_i and c_i is fixed, meaning we can express $\hat{\mathbf{t}}_{c_i}$ using the forward kinematics of this SP robot $p(\mathbf{t}_{e_i}^*, \tau_{0i}^*, \mathbf{v}_{0i}^*)$. Finally, \mathbf{X} is derived as the relative transformation between ${}^w\mathbf{T}_{e_i}$ and ${}^w\hat{\mathbf{T}}_{c_i}$. ■

C. Dual calibration robot

To represent the configuration of the dual calibration robot, we need the following variables

$$\begin{aligned} \{\mathbf{R}\} &:= \{\mathbf{R}_{c_i}, \mathbf{R}_{eb_i}, \mathbf{R}_{t_i}\}_m, \\ \boldsymbol{\tau} &:= \{\tau_{ea,c,i}, \tau_{eb,t,i}, \tau_{w,b,i}\}_m, \text{ and} \\ \mathcal{V} &:= \{\mathbf{v}_{ea,c,i}, \mathbf{v}_{eb,t,i}, \mathbf{v}_{w,b,i}\}_m, \end{aligned} \quad (58)$$

where \mathbf{R} are the rotation matrices corresponding to the reference frames of the camera and the end-effector of the second robot, $\boldsymbol{\tau}, \mathcal{V}$ are the prismatic variables for all of the SP robots in the dual calibration robot. These variables uniquely represent the configuration of the dual calibration robot in the sense that the pose of every reference frame on the robot can be represented as a function of (58) exclusively.

The goal of the calibration is to minimize

$$\hat{h}_2 := \sum_{i=1}^m \|\mathbf{A}_i \mathbf{X}_i \mathbf{B}_i - \mathbf{Y}_i \mathbf{C}_i \mathbf{Z}_i\|_F^2. \quad (59)$$

Observe that, for each sample i , (59) is the difference of the transformations obtained using the forward kinematics of two sub-trees of the kinematics chain of the dual calibration robot from the base to the target t . We develop the following cost function to model this difference.

$$f_2 := \sum_{i=1}^m (\|\mathbf{R}_{c_i} \mathbf{R}_{B_i} - \mathbf{R}_{t_i}\|_F^2 + \gamma \bar{p}_{fk}^2(\{\boldsymbol{\tau}, \mathcal{V}, \mathbf{R}\})) \quad (60)$$

The symbol γ is a weight to balance the terms. The function \bar{p}_{fk} is the difference of the translations following the forward kinematics, defined as

$$\begin{aligned} \bar{p}_{fk}^2 &:= \|p_{fk1} - p_{fk2}\|_2^2, \text{ where} \\ p_{fk1} &:= p(\mathbf{t}_{ea_i}, \tau_{ea,c,i}, \mathbf{v}_{ea,c,i}) + \mathbf{R}_{c_i} \mathbf{t}_{B_i}, \\ p_{fk2} &:= p(p(\mathbf{0}, \tau_{w,b,i}, \mathbf{v}_{w,b,i}) + \mathbf{R}_{eb_i} \mathbf{R}_{C_i}^\top \mathbf{t}_{C_i}, \tau_{eb,t,i}, \mathbf{v}_{eb,t,i}). \end{aligned} \quad (61)$$

We define the following kinematic problem for the calibration task.

Problem 9:

$$\min_{\boldsymbol{\tau}, \mathcal{V}, \{\mathbf{R}\}} f_2(\boldsymbol{\tau}, \mathcal{V}, \{\mathbf{R}\}) \quad (62a)$$

subject to $\forall i, i' = 1, \dots, m$:

$$\{\tau_{ea,c,i}, \mathbf{v}_{ea,c,i}, \mathbf{R}_{ea_i}, \mathbf{R}_{c_i}, \tau_{ea,c,i'}, \mathbf{v}_{ea,c,i'}, \mathbf{R}_{ea_{i'}}, \mathbf{R}_{c_{i'}}\} \in \mathcal{C}_{ft} \quad (62b)$$

$$\{\tau_{w,b,i}, \mathbf{v}_{w,b,i}, \mathbf{R}_{w_i}, \mathbf{R}_{b_i}, \tau_{w,b,i'}, \mathbf{v}_{w,b,i'}, \mathbf{R}_{w_{i'}}, \mathbf{R}_{b_{i'}}\} \in \mathcal{C}_{ft} \quad (62c)$$

$$\{\tau_{eb,t,i}, \mathbf{v}_{eb,t,i}, \mathbf{R}_{eb_i}, \mathbf{R}_{t_i}, \tau_{eb,t,i'}, \mathbf{v}_{eb,t,i'}, \mathbf{R}_{eb_{i'}}, \mathbf{R}_{t_{i'}}\} \in \mathcal{C}_{ft} \quad (62d)$$

Problem 9 minimizes the calibration goal (59) while enforcing the assumption (39) through the constraints (62b) - (62d).

D. Additional variables for constant transformations

To account for the quadratic constraints (48b) and (48c), we introduce the following variables.

$\mathbf{Y}_a := \{\mathbf{Y}_{a,i}\}_m$, where

$$\mathbf{Y}_{a,i} := \left\{ \begin{bmatrix} \hat{\mathbf{R}}_1^{(l_1)} \\ \mathbf{v} \\ 1 \end{bmatrix} \begin{bmatrix} \hat{\mathbf{R}}_1^{(l_1)} \\ \mathbf{v} \\ 1 \end{bmatrix}^\top \right\}_{l_1=1,2,3} \cup \left\{ \begin{bmatrix} \hat{\mathbf{R}}_2^{(l_1)} \\ \hat{\mathbf{R}}_2^{(l_2)} \\ 1 \end{bmatrix} \begin{bmatrix} \hat{\mathbf{R}}_2^{(l_1)} \\ \hat{\mathbf{R}}_2^{(l_2)} \\ 1 \end{bmatrix}^\top \right\}_{l_1=1,2,3, l_2=1,2} \quad (63)$$

The variable $\mathbf{Y}_{a,i}$ is a set of 9 7x7 matrices associated with the i -th configuration. Similar to \mathbf{Y}_i , each matrix in $\mathbf{Y}_{a,i}$ is also fixed-trace so long as $\hat{\mathbf{R}}_1, \hat{\mathbf{R}}_2 \in \text{SO}(3)$ and $\mathbf{v} \in \mathcal{S}^2$. For the dual calibration robot, the only unknown transformation of two reference frames with unknown poses is \mathbf{Z} . Explicitly, $\{\boldsymbol{\tau}, \mathbf{v}, \hat{\mathbf{R}}_1, \hat{\mathbf{R}}_2, \boldsymbol{\tau}', \mathbf{v}', \hat{\mathbf{R}}_{1'}, \hat{\mathbf{R}}_{2'}\}$ is linked to the robot as follows.

$$\begin{aligned} \hat{\mathbf{R}}_1 &= \mathbf{R}_{eb_i}, \hat{\mathbf{R}}_2 = \mathbf{R}_{t_i} \text{ and} \\ \boldsymbol{\tau} &= \tau_{eb,t,i}, \mathbf{v} = \mathbf{v}_{eb,t,i}, \forall i = 1, \dots, m. \end{aligned} \quad (64)$$

We define the following constraints to link \mathbf{Y}_a with these variables.

Definition 9: The additional-variable constraint $\mathbf{Y}, \mathbf{Y}_\tau, \mathbf{Y}_a \in \mathcal{C}_{av}$ is defined such that

- 1) (64) holds;
- 2) $\{\mathbf{M} \in \mathcal{Y} \mid \mathbf{M} \in \mathbf{Y}_{a,i}\}, \forall i = 1, \dots, m$.

As mentioned before, $\mathbf{R}_{eb_i}, \mathbf{R}_{t_i}$, and $\mathbf{v}_{eb,t,i}$ can be written as linear functions $g(\mathbf{Y})$ and $g_\tau(\mathbf{Y}_\tau)$. Item 1) of Definition 9 is enforced by having the r.h.s of (64) represented through these linear functions. Item 2) is to restrict the internal structure of $\mathbf{Y}_{a,i}$ through the same constraint \mathcal{Y} as \mathbf{Y}_i for they have a similar structure of outer products of stacked unit vectors.

VII. Simulation Results

A. Simulation settings

Throughout the simulations, we fix the following settings. The optimization problems are formulated using CVX [3], [6] and solved using MOSEK [15] and SDPT3 [19]. The SDPs are solved through Algorithm 1. For step 4, the cost of the rank-1 solution is improved using rank minimization (III-A), low-rank channel (Problem 5), and scheduling (14) interchangeably, following the fashion: Scheduling \rightarrow rank minimization \rightarrow Low rank channel \rightarrow rank minimization \rightarrow repeat. For the scheduling process, we use the following sequence of tolerances.

$$\{\sigma^k | \sigma^k = \max(10^{-5}, 1 - (1 + e^{(25-k)/5})^{-1})\}$$

This scheduling curve starts with a large tolerance that decreases rapidly; in practice, a similarly shaped linear curve yields comparable performance. Tuning of the parameters for the curve shape may result in different behaviors.

The iteration limits for each of the scheduling and low-rank channel phases are set as 1000 and 200, respectively. The sequence of scheduling and the low-rank channel is allowed to repeat once.

Along the iterations, we measure the following values for the quality of solutions.

- $\|\hat{\mathbf{R}}_a - \mathbf{R}_a^\top - \mathbf{I}\|$ is the error of a rotation \mathbf{R}_a from its ground truth value $\hat{\mathbf{R}}_a$.
- $\|\mathbf{t}_a - \hat{\mathbf{t}}_a\|$ is the error of a translation \mathbf{t}_a compared to its ground truth $\hat{\mathbf{t}}_a$.
- The eigenvalue gap (EG) defined by $\bar{\lambda} - \min(\lambda_1(\mathbf{Y}))$, representing the proximity of the rank-1 property.
- The duality gap (DG) defined by $f^* - d^*$, used as a certificate for global optimality.
- A solution is marked success when any of the rotational estimation error $\bar{\mathbf{R}} \geq 0.1$.

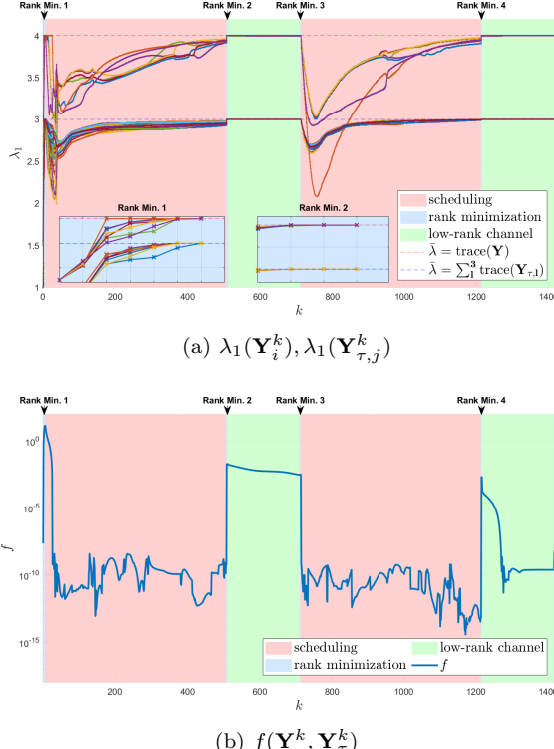


Fig. 4: Over the iterations of Algorithm 1, the rank is minimized in the rank minimization and scheduling phases, while the cost is reduced during the scheduling and the low-rank channel phases.

PnP estimation and Hand-eye calibration. We first evaluate the proposed method on two problems: camera pose estimation and hand-eye calibration. For camera pose estimation, a set of n target points and a camera pose are randomly generated, and the corresponding images of the targets are obtained. To simulate measurement noise, the image features are perturbed on the image plane in both x and y directions by a random displacement bounded by \hat{e}_p (pixels). For hand-eye calibration, the data are generated in the same manner, except the camera is mounted on a robot, and measurements are taken over m distinct configurations.

Dual-robot Calibration. To evaluate our method on the dual-robot calibration example, we simulate random motions of two robots: a Rethink Robotics Sawyer with a hand-mounted camera and a Kuka Iiwa 14 rigidly

holding a calibration target. The robot bases are fixed to the ground. For each selected pair of configurations, the camera measurements are generated from the relative transformation between the calibration target and the camera, after which noise is added to the measured transformations \mathbf{A} , \mathbf{B} , and \mathbf{C} .

For every problem, a TCSDP is constructed using the kinematics problems of the virtual robots. Then, the problem is solved through the proposed method. In the end, the transformations are recovered from the fixed-trace matrices.

B. Results

A solution process for the dual-robot calibration example is shown in Fig. 4, where the largest eigenvalues of the fixed-trace matrices are plotted in Fig. 4a and the cost variation in Fig. 4b. The results show that the low-rank channels reduce cost while keeping λ_1 close to $\bar{\lambda}$. During scheduling, the cost decreases as λ_1 first drops and then rises toward $\bar{\lambda}$ as the tolerance tightens. After each phase, rank minimization projects solutions onto the rank-1 set, typically causing a cost increase.

Tables III and IV report performance under varying measurement noise, showing higher average error and higher final cost with higher noise. In most cases, the solver converges to low-cost solutions; however, in a small fraction of cases, it fails to reach rank-1 low-cost solutions within the iteration limit, likely due to numerical issues or insufficient iterations. In successful cases, the eigenvalue gap is reduced under tolerance, showing the solutions are close to rank-1. In addition, a small average duality gap is observed, certifying global optimality.

VIII. Conclusion

We introduce the TCSDP, which enables gradient-based low-rank projection and optimality certification. A tailored solver is developed to obtain low-rank, low-cost solutions, with fixed-trace moment matrices designed for rotations and translations. Rank-1 solutions of these matrices allow exact recovery of the original manifold variables. We also present SP robot, a modular tool for modeling robotics problems via virtual robot kinematics, and demonstrate the full modeling–solving–certification pipeline on estimation and calibration tasks.

Future work includes accelerating the rank-minimization and cost-reduction procedure, as well as extending TCSDP to a broader range of robotics applications benefiting from convex optimization.

Appendix

A. Dual problem derivation

a) Unified primal problem.: We rewrite Problem 1 as

$$\min_{\{\mathbf{Y}_i \succeq \mathbf{0}\}} f(\mathbf{Y}) = \mathbf{y}^\top \mathbf{Q} \mathbf{y} + \mathbf{c}^\top \mathbf{y} + \text{constant} \quad (65a)$$

$$\text{s.t. } \mathcal{A}(\mathbf{Y}) = \mathbf{b}, \quad \mathbf{Y}_i \succeq \mathbf{0} \quad \forall i \in \{1, \dots, n\}. \quad (65b)$$

Problem	m	n	Noise Lv. \dagger	$\bar{\mathbf{R}}_c$	$\bar{\mathbf{t}}_c$	EG	DG	Cost	Time	Iterations	Success/ Total Runs
PnP	-	10	none	3.44e-05	1.05e-04	2.70e-05	6.13e-09	6.37e-10	3.89e+02	1.01e+03	19/20
	-	5	none	1.83e-05	6.11e-05	9.24e-05	4.22e-09	4.21e-09	2.97e+02	1.01e+03	20/20
	-	10	low	7.24e-03	2.38e-02	3.93e-05	1.22e-04	1.22e-04	4.39e+02	1.10e+03	19/20
	-	5	low	5.64e-03	1.99e-02	4.35e-06	5.40e-06	5.40e-06	3.02e+02	1.01e+03	20/20
	-	10	high	6.19e-03	2.02e-02	5.40e-05	1.08e-04	1.11e-04	8.48e+02	1.93e+03	20/20
Hand-Eye	6	9	none	1.82e-03	1.03e-03	1.04e-06	6.90e-07	6.88e-07	1.24e+03	1.22e+03	7/10
	6	9	low	5.32e-03	2.95e-03	-3.52e-06	1.85e-04	8.66e-04	2.53e+03	2.40e+03	7/10
	9	9	none	2.08e-03	1.13e-03	*	1.04e-06	*	2.38e+03	1.23e+03	9/10
	9	9	low	1.48e-02	1.07e-02	-1.37e-05	2.02e-03	2.68e-03	4.63e+03	2.34e+03	5/5
	9	9	high	1.27e-02	8.23e-03	-1.41e-05	2.11e-03	2.76e-03	4.61e+03	2.32e+03	5/5

\dagger none: $\hat{e}_p = 0$, low: $\hat{e}_p = 2$, high: $\hat{e}_p = 5$ | *:data pending

TABLE III: Average Estimation results of the PnP and hand-eye calibration problem

# Meas.	Noise Lv. \dagger	$\bar{\mathbf{R}}_x$	$\bar{\mathbf{R}}_y$	$\bar{\mathbf{R}}_z$	$\bar{\mathbf{t}}_x$	$\bar{\mathbf{t}}_y$	$\bar{\mathbf{t}}_z$	EG	DG	Cost	CPU Time \ddagger	Iterations	Success/ Total Runs
6	none	5.63e-03	2.39e-03	7.60e-03	4.57e-02	1.02e-02	3.94e-02	2.65e-06	*	2.42e-04	1.74e+04	1.59e+03	15/20
6	medium	9.89e-03	1.00e-02	1.22e-02	4.57e-02	1.28e-02	5.12e-02	6.59e-07	4.04e-04	5.40e-04	1.62e+04	1.64e+03	16/20
9	none	6.19e-05	2.69e-05	4.75e-05	4.85e-05	6.61e-05	4.79e-05	7.32e-07	7.57e-07	7.43e-09	1.83e+04	1.21e+03	19/20
9	low	2.03e-03	1.22e-03	2.27e-03	2.25e-03	1.18e-03	2.57e-03	1.32e-06	1.66e-05	1.58e-05	1.87e+04	1.21e+03	9/10
9	medium	5.04e-03	2.17e-03	5.03e-03	2.89e-03	2.44e-03	1.77e-03	7.33e-07	9.98e-05	1.16e-04	5.01e+03	1.59e+03	9/10
9	high	1.28e-02	5.01e-03	1.24e-02	8.90e-03	8.50e-03	1.29e-02	7.10e-07	8.86e-04	1.31e-03	3.96e+04	2.42e+03	17/20

*: data pending

\dagger low: $(\theta, l) = (0.1^\circ, 1e-4)$, medium: $(\theta, l) = (0.3^\circ, 3e-4)$, high: $(\theta, l) = (0.8^\circ, 8e-4)$. Noise added by $\bar{\mathbf{R}} = \mathbf{R}_{\text{rot}}(\mathbf{v}, \text{rand}(0, \theta))$, $\bar{\mathbf{t}} = \mathbf{t} + \text{rand}(-l, l)$.

\ddagger The CPU computation time measured for all CPU cores. Real clock time is approximately CPU time divided by the number of CPU cores.

TABLE IV: Average Calibration results of the dual robot system

Here \mathcal{A} is a given linear operator acting on the block tuple \mathbf{Y} , and \mathbf{b} is given. This includes all of the linear (including trace) constraints in Problem 1.

b) Epigraph reformulation (linear objective + LMI).: Let $\mathbf{Q} = \mathbf{L}^\top \mathbf{L}$ be a Cholesky (or any) factorization and introduce an epigraph variable $t \in \mathbb{R}$. Since $\mathbf{y}^\top \mathbf{Q} \mathbf{y} = \|\mathbf{L} \mathbf{y}\|_2^2$, the inequality $t \geq \mathbf{y}^\top \mathbf{Q} \mathbf{y}$ admits the Schur-complement LMI

$$\begin{bmatrix} t & (\mathbf{L} \mathbf{y})^\top \\ \mathbf{L} \mathbf{y} & \mathbf{I} \end{bmatrix} \succeq \mathbf{0},$$

where \mathbf{I} is the identity of conformable size. Dropping the additive constant in (65a) (it does not affect optimal \mathbf{Y}), the problem is equivalent to

$$\min_{\{\mathbf{Y}_i \succeq \mathbf{0}\}, t} t + \mathbf{c}^\top \mathbf{y} \quad (66a)$$

$$\text{s.t. } \mathcal{A}(\mathbf{Y}) = \mathbf{b}, \quad \mathbf{Y}_i \succeq \mathbf{0} \quad \forall i, \quad (66b)$$

$$\begin{bmatrix} t & (\mathbf{L} \mathbf{y})^\top \\ \mathbf{L} \mathbf{y} & \mathbf{I} \end{bmatrix} \succeq \mathbf{0}. \quad (66c)$$

This is a standard-form SDP with a linear objective and affine LMI constraints in (\mathbf{Y}, t) .

c) Dual derivation.: Introduce dual variables:

- $\boldsymbol{\rho}$ for the equality constraints $\mathcal{A}(\mathbf{Y}) = \mathbf{b}$,
- $\{\mathbf{S}_i \succeq \mathbf{0}\}$ for $\mathbf{Y}_i \succeq \mathbf{0}$,
- $\mathbf{Z} \succeq \mathbf{0}$ for the LMI (66c), partitioned as $\mathbf{Z} = \begin{bmatrix} \alpha & \mathbf{z}^\top \\ \mathbf{z} & \mathbf{Z}_{22} \end{bmatrix}$, where $\alpha \in \mathbb{R}$, $\mathbf{z} \in \mathbb{R}^r$ and $\mathbf{Z}_{22} \in \mathbb{S}^r$ with r the row dimension of \mathbf{L} .

The Lagrangian of (66a)–(66c) is

$$\begin{aligned} \mathcal{L}(\mathbf{Y}, t; \boldsymbol{\rho}, \{\mathbf{S}_i\}, \mathbf{Z}) = & (t + \mathbf{c}^\top \mathbf{y}) + \boldsymbol{\rho}^\top (\mathbf{b} - \mathcal{A}(\mathbf{Y})) - \sum_{i=1}^n \langle \mathbf{S}_i, \mathbf{Y}_i \rangle \\ & - \left\langle \mathbf{z}, \begin{bmatrix} t & (\mathbf{L} \mathbf{y})^\top \\ \mathbf{L} \mathbf{y} & \mathbf{I} \end{bmatrix} \right\rangle. \end{aligned} \quad (67)$$

Using the block structure of \mathbf{Z} ,

$$\left\langle \mathbf{z}, \begin{bmatrix} t & (\mathbf{L} \mathbf{y})^\top \\ \mathbf{L} \mathbf{y} & \mathbf{I} \end{bmatrix} \right\rangle = \alpha t + 2 \mathbf{z}^\top \mathbf{L} \mathbf{y} + \text{tr}(\mathbf{Z}_{22}).$$

Hence

$$\begin{aligned} \mathcal{L} = & (1 - \alpha) t + (\mathbf{c} - 2 \mathbf{L}^\top \mathbf{z})^\top \mathbf{y} + \boldsymbol{\rho}^\top \mathbf{b} - \langle \mathcal{A}^*(\boldsymbol{\rho}), \mathbf{Y} \rangle \\ & - \sum_{i=1}^n \langle \mathbf{S}_i, \mathbf{Y}_i \rangle - \text{tr}(\mathbf{Z}_{22}), \end{aligned} \quad (68)$$

where \mathcal{A}^* is the adjoint of \mathcal{A} and $\langle \mathcal{A}^*(\boldsymbol{\rho}), \mathbf{Y} \rangle := \sum_{i=1}^n \langle (\mathcal{A}^*(\boldsymbol{\rho}))_i, \mathbf{Y}_i \rangle$.

For the dual function g , take the infimum over (\mathbf{Y}, t) . This is finite iff the coefficients of t and of each \mathbf{Y}_i vanish:

$$\alpha = 1, \quad (69)$$

$$\mathcal{V}^*(\mathbf{c} - 2 \mathbf{L}^\top \mathbf{z}) - \mathcal{A}^*(\boldsymbol{\rho}) - \mathbf{S} = \mathbf{0}, \quad (70)$$

where $\mathbf{S} := \{\mathbf{S}_i\}_{i=1}^n$, and $\mathcal{V} : \mathbf{Y} \mapsto \mathbf{y} = \text{vec}(\mathbf{Y})$ and \mathcal{V}^* is its adjoint, i.e., $\langle \mathcal{V}^*(\mathbf{r}), \mathbf{Y} \rangle = \mathbf{r}^\top \text{vec}(\mathbf{Y})$ for any $\mathbf{r} \in \mathbb{R}^N$. Under (69),(70), the infimum equals $\boldsymbol{\rho}^\top \mathbf{b} - \text{tr}(\mathbf{Z}_{22}) = \boldsymbol{\rho}^\top \mathbf{b} - \text{tr}(\mathbf{Z}) + 1$. Therefore, the dual SDP is exactly Problem 3

References

- [1] A. Agrawal and K. Sreenath. Discrete control barrier functions for safety-critical control of discrete systems with application to bipedal robot navigation. In Robotics: Science and Systems, volume 13. Cambridge, MA, USA, 2017.
- [2] A. I. Barvinok. Problems of distance geometry and convex properties of quadratic maps. Discrete & Computational Geometry, 13(1):189–202, 1995.
- [3] I. CVX Research. CVX: Matlab software for disciplined convex programming, version 2.0. <https://cvxr.com/cvx>, Aug. 2012.
- [4] F. Dümbgen, C. Holmes, B. Agro, and T. Barfoot. Toward globally optimal state estimation using automatically tightened semidefinite relaxations. IEEE Transactions on Robotics, 40:4338–4358, 2024.
- [5] M. A. Fischler and R. C. Bolles. Random sample consensus: a paradigm for model fitting with applications to image analysis and automated cartography. Communications of the ACM, 24(6):381–395, 1981.

- [6] M. Grant and S. Boyd. Graph implementations for nonsmooth convex programs. In V. Blondel, S. Boyd, and H. Kimura, editors, *Recent Advances in Learning and Control, Lecture Notes in Control and Information Sciences*, pages 95–110. Springer-Verlag Limited, 2008. http://stanford.edu/~boyd/graph_dcp.html.
- [7] R. I. Hartley and A. Zisserman. *Multiple View Geometry in Computer Vision*. Cambridge University Press, second edition, 2004.
- [8] C. Helmberg and F. Rendl. A spectral bundle method for semidefinite programming. *SIAM Journal on Optimization*, 10(3):673–696, 2000.
- [9] J. B. Lasserre. Global optimization with polynomials and the problem of moments. *SIAM Journal on optimization*, 11(3):796–817, 2001.
- [10] Z.-Q. Luo, W.-K. Ma, A. M.-C. So, Y. Ye, and S. Zhang. Semidefinite relaxation of quadratic optimization problems. *IEEE Signal Processing Magazine*, 27(3):20–34, 2010.
- [11] Y. Ma. *An invitation to 3-D vision: from images to geometric models*. Springer, 2004.
- [12] J. R. Magnus. On differentiating eigenvalues and eigenvectors. *Econometric Theory*, 1:179–191, 1985.
- [13] N. H. A. Mai, J.-B. Lasserre, and V. Magron. A hierarchy of spectral relaxations for polynomial optimization. *Mathematical Programming Computation*, 15(4):651–701, 2023.
- [14] N. H. A. Mai, J. B. Lasserre, V. Magron, and J. Wang. Exploiting constant trace property in large-scale polynomial optimization. *ACM Transactions on Mathematical Software*, 48(4):1–39, 2022.
- [15] MOSEK ApS. The MOSEK optimization toolbox for MATLAB manual. Version 10.0., 2022.
- [16] J. Nie. Optimality conditions and finite convergence of lasserre’s hierarchy. *Mathematical programming*, 146(1):97–121, 2014.
- [17] G. Pataki. On the rank of extreme matrices in semidefinite programs and the multiplicity of optimal eigenvalues. *Mathematics of Operations Research*, 23(2):339–358, 1998.
- [18] A. Shapiro. Rank-reducibility of a symmetric matrix and sampling theory of minimum trace factor analysis. *Psychometrika*, 47(2):187–199, 1982.
- [19] K.-C. Toh, M. J. Todd, and R. H. Tütüncü. Sdpt3—a matlab software package for semidefinite programming, version 1.3. *Optimization methods and software*, 11(1-4):545–581, 1999.
- [20] H. Waki, S. Kim, M. Kojima, and M. Muramatsu. Sums of squares and semidefinite program relaxations for polynomial optimization problems with structured sparsity. *SIAM Journal on Optimization*, 17(1):218–242, 2006.
- [21] J. Wang, V. Magron, and J.-B. Lasserre. Chordal-tssos: a moment-sos hierarchy that exploits term sparsity with chordal extension. *SIAM Journal on optimization*, 31(1):114–141, 2021.
- [22] L. Wu and R. Tron. An SDP optimization formulation for the inverse kinematics problem. In 2023 62nd IEEE Conference on Decision and Control (CDC), pages 4731–4738, 2023.
- [23] L. Wu and R. Tron. IKSPARK: An inverse kinematics solver using semidefinite relaxation and rank minimization. *arXiv preprint arXiv:2403.12235*, 2024.
- [24] L. Wu and R. Tron. Visual inverse kinematics: Finding feasible robot poses under kinematic and vision constraints. In 2025 American Control Conference (ACC), pages 3751–3757. IEEE, 2025.
- [25] H. Yang and L. Carlone. Certifiably optimal outlier-robust geometric perception: Semidefinite relaxations and scalable global optimization. *IEEE transactions on pattern analysis and machine intelligence*, 45(3):2816–2834, 2022.
- [26] H. Yang, J. Shi, and L. Carlone. TEASER: Fast and certifiable point cloud registration. *37(2):314–333*, 2020.
- [27] A. Yurtsever, J. A. Tropp, O. Fercoq, M. Udell, and V. Cevher. Scalable semidefinite programming. *SIAM Journal on Mathematics of Data Science*, 3(1):171–200, 2021.